

Computational Foot Modeling: Scope and Applications

Enrique Morales-Orcajo^{1,2,3} · Javier Bayod^{1,2} · Estevam Barbosa de Las Casas³

Received: 26 February 2015 / Accepted: 6 March 2015 / Published online: 14 March 2015
© CIMNE, Barcelona, Spain 2015

Abstract The aim of this paper is to provide a general review of the computational models of the human foot. The field of computational simulation in biomechanics has significantly advanced in the last three decades. Medicine and engineering fields increasingly collaborate to analyze biological systems. This study seeks a link between two areas of knowledge to achieve a better understanding between clinicians and researchers. The review includes two-dimensional and three-dimensional, detailed and simplified, partial- and full-shape models of the lower limb, ankle and foot. Practical issues in computational modeling, tissue constitutive model approaches and pioneering applications are extensively discussed. Recent challenges and future guidelines in the field of foot computational simulation are outlined. Although this study is focused on foot modeling, the main ideas can be employed to evaluate other parts of the body. The advances in computational foot modeling can aid in reliable simulations and analyses of foot pathologies, which are promising as modern tools of personalized medicine.

1 Introduction

Feet are some of the most complex structures in the human body; they consist of small bones connected by cartilages and ligaments, which maintain structural integrity, several muscles, which conduct movements, and fat tissue and heel pads, which absorb impacts. They are responsible for supporting the weight of the entire body and balancing forces during human locomotion [1]. Due to their arched structure, they respond to an extensive range of activities, such as walking, running, jumping, and climbing. However, human feet are often neglected when the lower limb or entire body is analyzed and are treated as a single body while disregarding the complex structure that achieves superior mechanical responsiveness.

Due to this complexity, the feet must be simulated to understand how they function. Medical imaging, external measurements and cadaveric dissections are insufficient for understanding the role of each internal structure during gait. In this regard, computational simulations and, in particular, the finite element (FE) method is the most popular and accepted method for predicting the behavior of structural and mechanical systems for performance analysis [2, 3]. The significant progress in computational simulation and computing power of current computers constitutes a successful tool for biomechanical research to analyze irregular geometries with complex boundary conditions and advanced material properties. These simulations provide important clinical information, which is difficult to measure with experimental procedures. From a podiatric point of view, models of the human foot and lower extremity have already been pointed out as one of the most important directions for predicting structural behavior of their components [4]. The knowledge obtained from

✉ Estevam Barbosa de Las Casas
estevam.lascasas@gmail.com; estevam@dees.ufmg.br

¹ Group of Structural Mechanics and Materials Modeling (GEMM), Aragon Institute of Engineering Research (I3A), University of Zaragoza, Zaragoza, Spain

² Biomedical Research Networking Center in Bioengineering, Biomaterials and Nanomedicine (CIBER-BBN), Zaragoza, Spain

³ Group of Biomechanical Engineering UFMG - (MecBio), School of Engineering, Universidade Federal de Minas Gerais, Av. Antônio Carlos 6627, Bloco I sala 4116, Belo Horizonte, MG CEP 31270-901, Brazil

simulations aids in the diagnosis, treatment and prevention of foot pathologies.

The challenge of computational simulation of the foot/ankle complex began in 1981. Nakamura et al. [5] presented a simplified and idealized model of the foot and shoe during midstance. The next model that appeared in the literature was a two-dimensional (2D) foot skeleton, which was employed to analyze the stresses during three walking phases [6]. Although the model by Patil et al. did not simulate the soft tissue compared with the model by Nakamura et al., it considered the properties of cartilages and ligaments. In 1997, Lemmon et al. [7] published an investigation of the alterations in pressure under the second metatarsal head as a function of insole thickness and tissue thickness. Although this model only represented a sagittal section through the second metatarsal bone, their approach considered hyperelastic properties of the foot soft tissue; it was significant and extensively cited. Gefen's studies provided significant advances in the description of the stress distribution for several subphases of stance, which established the groundwork in material properties, loads and constraints of foot FE models [8–10].

In the early 2000s, three-dimensional (3D) foot models were developed with important simplifications. Jacob's oversimplified model, which treated the lateral metatarsals and the medial metatarsals as single bodies [11] was one such model. Other authors simplified the geometry by affixing the midfoot and forefoot joints [12, 13]. Cheung's studies [14, 15] facilitated the use of 3D foot models for analyzing internal stress and strain distributions of the foot structure. Based on the boundary conditions and material properties proposed by these researchers, a large number of foot models with more accurate geometries were used in many different applications in recent years.

The objective of this paper is to provide a general review of the computational models of the human foot. 2D and 3D, detailed and simplified, partial- and full-shape models of the lower limb, ankle and foot were included in the review. A comprehensive overview of geometry reconstruction procedures and some issues in computational foot modeling are discussed in Sect. 2. The constitutive models for hard and soft tissues of the foot are briefly discussed in Sect. 3. A critical review of foot computational studies is presented in Sect. 4. Recent challenges and future guidelines in the field are detailed in Sect. 5. The main conclusions of the study are listed in Sect. 6.

This paper surveys the computational simulation of the human foot, explores the challenges and possibilities for the simulation of medical issues and helps clinicians to better understand the computational predictions. It serves as a link between two disciplines that increasingly collaborate. Although the study is focused on foot models, the general concepts can be extrapolated to other parts of the

body, such as the hand, shoulder, hip or knee. The foot is a complete reference considering that it involves many different and interconnected tissues and compounds that work together.

2 Foot Model Development

Model reconstruction, the characterization of tissues and the determination of boundary conditions are the most complex steps in FE analysis. To address these problems, a methodology should be followed, as outlined in Fig. 1 and described in the next section.

2.1 Geometry and Mesh Reconstruction

The geometry of the foot in a FE model is generally obtained from 3D reconstruction of computer tomography (CT) or magnetic resonance imaging (MRI), which can be obtained from dataset libraries [8, 16, 17] or scanned patients [18–20]. In the literature, CT and MRI are equally cited. Both techniques are painless and noninvasive; the main difference between the two techniques is that CT accurately outlines bone inside the body, whereas MRI provides much finer soft tissue detail, as shown in Fig. 2. For the patient, CT scanning can pose a small risk of irradiation, especially by prolonged exposure; however, no biological hazards have been reported with the use of MRI.

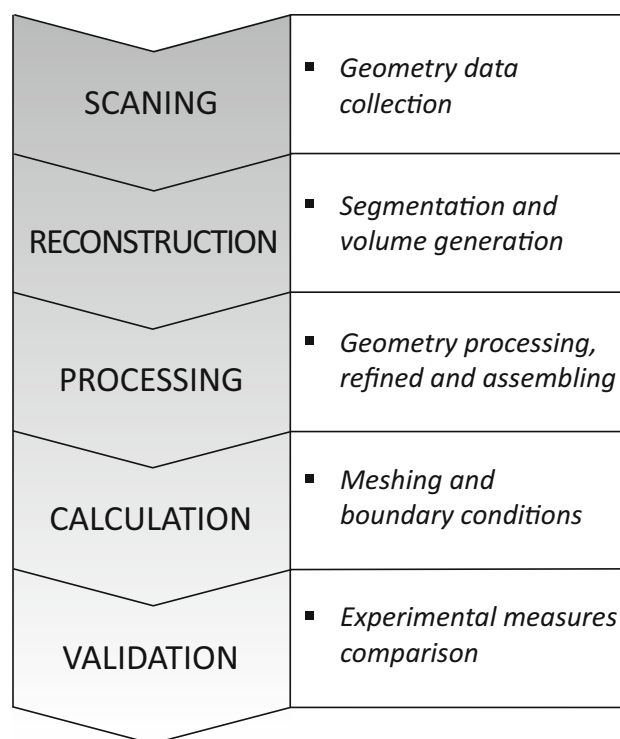
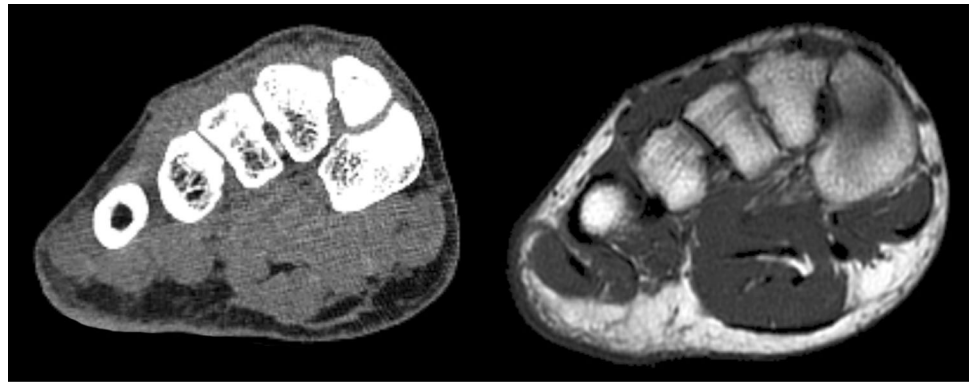


Fig. 1 Computation model developing process diagram

Fig. 2 *Left image:* CT image of midfoot. *Right image:* MRI of midfoot



From a practical viewpoint, less time is required for total testing in CT whereas MRI can change the imaging plane without moving the patient.

The individual volumes of each compound are created by the segmentation process, 2D slice information is retrieved for 3D reconstruction. The volumes generated from the segmentation are frequently refined in a CAD program to accomplish a good fit between hard and soft tissue; small gaps, sharp edges or other disruptions that may unnecessarily complicate the mesh are prevented. It is also used to add objects such as insoles, implants and ground blocks for specific applications. These volumes are exported to a FE program to perform the analysis. In this step, the geometry is meshed and loads, constraints and material properties are defined.

A large variety of software for image reconstruction, geometry processing and FE calculation are available. The most popular medical image processing software for 3D generation from DICOM files is MIMICS[®] (Materialise, Leuven, Belgium) [21, 22], SIMPLEWARE[®] (Simpleware Ltd., Exeter, UK) [23] and AMIRA[®] (Mercury Computer Systems, Germany) [24]; the segmentation process is occasionally performed with custom-made codes [25–27]. The models that require extra editing to improve model accuracy or to smooth surfaces were processed by SOLIDWORKS[®] (Dassault Systemes, SolidWorks Corp., USA) [28, 29]. Regarding FE packages, ABAQUS[®] (ABAQUS Inc., Pawtucket, RI, USA) and ANSYS[®] (ANSYS Inc., Canonsburg, PA, USA) are the most cited software. They are employed in more than 60 % of the papers published on FE analyses of the foot; LS-DYNA[®] (LSTC, Livermore, CA, USA), PATRAN[®] (MSC., Santa Ana, CA, USA) and MSC.MARC[®] (MSC.software corporation, Santa Ana, CA, USA) are also commonly reported (Table 1).

2.2 Verification and Validation

The ultimate objective of a biomechanical simulation is to obtain reliable results that can be used to develop clinically

Table 1 Percentage of papers that employed each FE package on the literature of computational analyses of the foot

ABAQUS [®]	45 %
ANSYS [®]	17 %
PATRAN [®]	6 %
LS-DYNA [®]	6 %
MARC [®]	6 %
OTHERS	20 %

relevant recommendations. The opinions about the limits of these simulations and their conclusions significantly differ. Some researchers consider computational simulation to be acceptable from a practical engineering perspective because it provides statistically meaningful predictions [30]. Other researchers suggest that numerical models are inherently false [31]. Despite the diverse viewpoints, models have exponentially increased in the last three decades [32] due to the potential applications of this tool and the fact that modeling reduces complicated clinical testing. To raise the credibility of their predictions, models must be verified and validated and all relevant aspects must be discussed [33].

Verification measures how close a result is to the exact solution. Validity evaluates whether mathematical descriptions of structural aspects mimic a real problem. In the field of solid biomechanics, verification usually consists of implementing constitutive equations and assessing resulting errors. This verification is probably due to the fact that most biomechanics studies use established and/or commercially available computational software for which code verification has already been completed [34]. However, validation must be assessed by experimental tests and requires a long process that involves the entire scientific community (scientists, engineers and clinicians) [35]. Henninger et al. [36] described two predominant types of validation: direct validation and indirect validation. In direct validation, the experiment is specifically designed for the validation of the proposed model. In indirect validation, a comparison of the model predictions with previous studies, in which the settings of the experiment cannot be

controlled by the user, is performed. Both processes appear in the literature of FE analyses of the foot.

Regarding the validation of foot models, the most common process to validate FE results is the comparison between predicted plantar pressure and measured plantar pressure. The most prevalent plantar pressure measurement systems are platform systems and in-shoe systems [37, 38]. In this process, the matching parameters include the entire plantar pressure distribution [22], the peak plantar pressure of each region [39], the total contact area [27] or the ground reaction force along the stance phase [40]. The peak plantar pressure that is predicted by FE models is generally higher than the measured peak pressure [15, 41, 42]. This deviation is primarily attributed to different resolutions between the scan system and the model. The measuring system reports an average pressure for the area of the sensor; a minimum average pressure of 25 mm² has been suggested to prevent underestimations [37]. The FE model provided values for an area between 1 and 5 mm² depending on the mesh size. The maximum plantar pressure predicted by the FE model is expected to exceed the pressure measurements with the platform. This discrepancy may be influenced by the fact that some authors compared the measured plantar pressure with the von Mises stress predicted by FE model. These values do not apply the same concept because the von Mises stresses include hydrostatic and deviatoric stresses. Thus, the comparison with the plantar pressure prediction reduces this overestimation.

When the comparison with the plantar pressure is not feasible because the model does not include fat tissue, the validation parameters consist of bone displacement and arch deformation. The validation can be performed using radiographic images [24] or by cadaveric experiment [43]. Post-surgery studies or treatment simulations can be compared with cadaveric studies or clinical reports [9, 41, 44]. Computational values have also been validated by measuring soft tissue deformation [45]. Another method used to assess the model involves computationally replicating the experiments and comparing the results, for example, the impact test [46, 47] or kicking a ball [48]. A good practice for ensuring the reliability of model predictions is a comparison of the results with different measurements for different load conditions [49, 50] and the use of different FE models for different patient/donor experiments [51]. This practice is especially important for clinical applications, in which the validation process should be much more exhaustive, because the predictions enable direct application in patients. Any parameter that can be used for computational predictions and experimental measurements is suitable for validating a FE model.

Although the validation must be performed by authors, detailed information about the quality of the mesh [52] and the characteristics of the model [32] should be provided

when a study is based on a FE analysis to ensure that the reader will be able to assess the value of the results and accept its predictions. According to Oberkampff et al. [53], engineering does not require the ‘absolute truth’ but a statistically meaningful comparison of computational and experimental results, which are designed to assess random (statistical) and bias (systematic) errors. Computational models in biomechanics are habitually developed to simulate phenomena that cannot be experimentally measured and require model inputs that are unknown or may vary by several orders of magnitude. Although the predictions cannot be directly compared, computational models may provide valuable insight into the mechanical behaviors of complex biological systems, such as feet, if the verification is properly performed.

3 Foot Tissue Properties

The simulation of biological tissues is a fascinating challenge because they exhibit complex characteristics. They have a fibrous structure with a specific spatial orientation and an anisotropic mechanical response. Biological tissues are multiphasic with a fluid phase and a solid matrix. Many biological tissues experience a strong nonlinear behavior, such as large deformations (hyperelastic behavior) and a time-dependent nature (viscoelastic behavior). Generally, they display patterns of hysteresis and their responses vary with load application speed. As living tissue, they experience intersubject variability, sexual differentiation, age-dependency; they evolve according to solicitations, diseases or different types of cell activities [54].

Fortunately, engineers employ tools, such as arrangements, assumptions and simplifications, which help them to address these complexities. In the sequence, a brief summary of the main numerical approaches and the approved parameters of foot tissues that are used in computational studies are provided.

At the foot level and from a biomechanical perspective, only the connective and muscular tissues are included in the models. Connective tissues give shape to organs and hold them in place, whereas muscular tissue actively produces force and causes motion within internal organs. Epithelial tissue and nervous tissue are not considered for mechanical analysis. Biological tissues contain two types of tissues: hard and soft tissues. The main difference is the existence of the inorganic phase. This mineral component makes hard tissue stiffer and more resistant than soft tissue, as shown in Fig. 3. Figure 3 depicts the behaviors of the tissues in a uniaxial traction test until the failure point. During physiological performance, tissues are expected to function in the lower half of their curves. Figure 4 shows the stress–strain curve of the foot tissues that function

under compression loads. These graphs are presented as a qualitative comparison between the mechanical behaviors of the different healthy tissues that are involved in foot computational analysis; however, these curves can quantitatively vary depending on the speed load application.

3.1 Hard Tissues

The biological tissue that incorporates minerals into soft matrices, which generally form a protective shield or structural support, is classified as hard tissue. This group includes bones, horns and shells. The foot only contains osseous material.

Bony tissue is one of the strongest and most rigid structures of the body due to its combination of inorganic and organic elements. It achieves very high mechanical performance because the minerals, calcium and phosphate

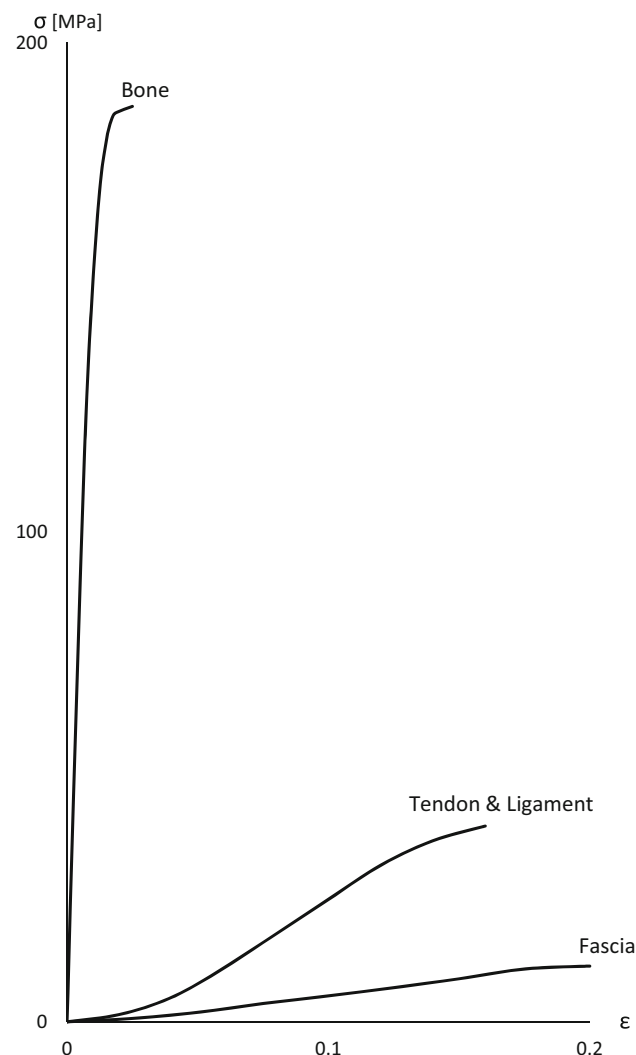


Fig. 3 Stress-strain curves of the foot tissues that function under traction loads

confer stiffness and stretch in compression and soft organic materials, such as collagen, proteoglycans and proteins, contribute to traction properties. Bone is an anisotropic material that exhibits different behaviors under tension and compression [55]. It is composed of cortical bone and trabecular bone; the latter has the lower elastic modulus [56].

3.1.1 Bone

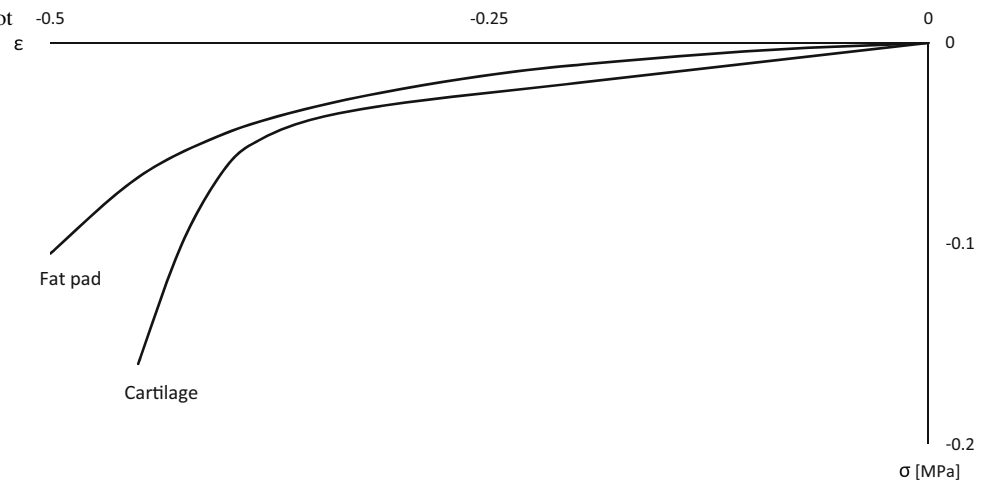
Dense compact bone is referred to as cortical bone, is located on the cortex, which is the outer shell of bone. It is harder, stronger and stiffer than cancellous bone and contributes to approximately 80 % of the weight of a human skeleton. The mechanical properties of the cortical tissue vary depending on the orientation of the specimen (longitudinal, medial–lateral, and anterior–posterior) [57]. Due to the complexity of this material in computational simulations, it is frequently assumed to be homogeneous, isotropic and linear elastic. These assumptions were investigated by Huijkes [58], who reported that cortical and trabecular bones may be considered to exhibit linearly elastic behaviors in the quasi-static loading case. The most predominant value of Young's modulus for cortical bone is 17 GPa [20, 47, 59]. The literature contains limited data regarding the mechanical properties of foot bones; thus, the properties that are utilized in foot models are estimated with mean values of leg bones [60]. This comparison is reasonable because the modulus of elasticity measurements for both the leg and the arm fall within the same range [61].

Generally, biological materials are discontinuous to any level but cancellous bone is also discontinuous on a macroscopic level; thus, it resembles a structure instead of a material. The orientation and density of the trabecular structure are important factors in the mechanical behavior of spongy bone [62]. A dependence of the mechanical properties of cancellous bone on the anatomic location and function of the tested bony region is observed [63, 64], that is, bones adapt to their mechanical environment [65]. Keaveny et al. [66] reported that trabecular bone exhibits a completely linear elastic behavior and yields at low strains. Due to these features, the estimated values for the Young's modulus of trabecular bone material range from 0.1 to 20 GPa [67, 68]. Current studies have indicated considerably lower values for Young's modulus.

Regarding foot models, the few authors who consider the properties of the trabecular bone use these lower values, which range from 0.4 to 0.7 GPa [12, 47, 69], with 5.5 GPa as the highest value [70]. A Poisson's ratio of 0.3 has been reported for both cortical and trabecular bone in all tests.

The elastic properties of bone can also be defined by the mathematical relationship with bone density using gray

Fig. 4 Stress-strain curves of the foot tissues that function under compression loads



scale values of computer topographies. In the scientific literature, a large number of mathematical relationships between the densitometric measurements and Young's modulus with extensive scatter are identified [71]. This finding may be attributed to the difficulty of measuring the properties of trabecular bone. In any case, this procedure has not been applied to subject-specific FE foot models. Bandak et al. [12] utilized one of these formulas to determine the elastic modulus of spongy bone but they did not use it to apply a progressive transition of the Young modulus between both types of bone. A recently published metatarsal FE study employed an inhomogeneous (density dependent) Young's modulus for bone [51]. They postulated that the distribution of the different material properties of the metatarsal significantly affected the mechanical response. They also compared the mean difference in the strains between the FE models with inhomogeneous properties with three distinct constant values that are commonly found in the literature. The authors conclude that a specific constant Young's modulus may adequately represent a particular metatarsal, whereas the same constant Young's modulus may result in poor agreement with other metatarsal bones.

The most common simplification of the simulation of the foot osseous structure involves treating it as a homogeneous, isotropic, and linear elastic material. The elastic modulus and Poisson's ratio of this equivalent material is assumed to be 7.3 GPa and 0.3, respectively. This value was obtained by Nakamura et al. [5], who justified it as a frequent value in the literature; however, they did not provide any source or justification for this value. The most cited authors in foot FE modeling [9, 72] defended this value as a weighted average of cortical and trabecular elasticity properties. Despite the apparent lack of validation, this idealization is accepted by the majority of authors who continue to use these properties. A slightly higher

value of 10 GPa for the Young's modulus for the bone block was employed by some authors [7, 73] based on Van Buskirk and Ashman studies [74]; however, this value has not been recently utilized. A recent study of the effect of Young's modulus on the simulation of a foot FE model consisted of a comparison between a computer simulation and an in vitro experiment, which yielded values that were four times higher than the traditional Young's modulus. The value of 29.2 GPa for the Young modulus of foot and ankle bones showed better agreement with the measurements of surface strain in an in vitro experiment of six cadaveric feet [75].

Some studies assume foot bones as rigid bodies [47]. In these studies, the internal stress is not considered to be a variable and the objective of the study is the motion of the bones (joint kinetics). This approximation is even more simplistic than the homogenous bone; it is justified by the fact that the bone has a much greater stiffness than soft tissues Fig. 3. This assumption can only be accepted in particular cases, when the objective of the study is the stress of the surrounding tissues due to the motion of the foot joints.

Shoulder [76], elbow [77], finger [78], pelvis [79] and knee [80] FE models tend to distinguish both materials because the complexity of the bony structure and the size and number of bones in these parts is simpler compared with the foot, where achieving the convergence of the model and computer time are significant problems. As a result, uniform mechanical properties are used to analyze the mechanical behavior of the foot skeleton.

In 2009, Garcia-Aznar et al. [69] compared the displacement and stresses of a foot skeleton FE model using two different methodologies. They noted that the deformed shape in both models was similar; however, they detected an important underestimation of the maximum stress level when homogeneous bone was considered. Therefore, this

assumption may be suitable for foot applications that focus on the adipose tissue surrounding a foot skeleton, such as plantar pressure estimation and footwear design problems. However, an analysis of bone functions is inaccurate.

The current trend, which is aided by continuous advancements in numerical techniques and computer technology, features the use of refined models that not only distinguish between cortical and trabecular bone but also include more complex simulations that consider anisotropic and hyperelastic behaviors.

3.2 Soft Tissues

Soft tissue connects, supports, or surrounds other structures and organs of the body. It is a composite that consists of a very flexible organic matrix that is strengthened by collagen and elastin fibers. Soft tissues in the feet include cartilage, ligament, fascia, tendon, muscle, skin, artery and vein. Blood vessels are not considered in the mechanical analysis.

The behavior of soft tissue is dependent on its composition and structure, particularly with regard to the percentage of fibers, its features, the directionality and the type of grouping. Thus, the tissues that are specialized in tensile stresses, such as tendons and ligaments, are rich in fibers that are oriented in the direction of the stress, whereas the tissues that can withstand compressive forces, such as cartilage rich in proteoglycans with fiber, are randomly distributed. They regularly support large deformations and are highly anisotropic. They are quasi-incompressible in an extensive range of deformations.

3.2.1 Cartilage

Cartilage is a relatively soft tissue that is present in many parts of the body, such as nose, ear, and joints; this review focuses on articular cartilage. Specifically, articular cartilage covers the ends of bones to facilitate load carriage and lubrication. Its structure can withstand enormous compressive forces and it is capable of creating a low friction surface on which joints glide [81]. This tissue can be considered to be highly heterogeneous, anisotropic and multiphasic and primarily consists of water, collagen fibrils and a dense skein of negatively charged proteins—the proteoglycans.

Similar to other biological tissues, an extensive variety of numerical approaches exists to represent the constitutive behavior of articular cartilage, which includes elastic, viscoelastic, poroelastic, electro-mechanic, fibril-reinforced, bi-component, biphasic, and three-phased behaviors [81]. However, the complete spectrum of the tissue's complex responses is not recovered in a unique model. The appropriateness of each approach is dependent on the

specific case to analyze. In foot modeling, which includes many joints, articular cartilage tissue is considered to be an isotropic linear elastic material with no interstitial fluid flow during the steady-state phase. Clift [82] noted that under short-term or instantaneous loading, cartilage should be modeled as a linear elastic material. This approach reduces the complexity of the calculations without losing accuracy because the volume of cartilage and its influence in the final result is almost negligible when compared with other tissues of the foot.

Two basic pathways can be employed to simulate the articular behavior: (a) to fill the articular gap with a solid to simulate the flexibility of the connection between bony structures [8, 83, 84] or (b) to consider the surface–surface interaction with frictionless contact elements. In this case, bones are allowed to slide over each other with the constraints governed by the congruent facets and ligamentous structures [41, 44, 72]. Regarding the accuracy of the approximation, the second pathway is slightly better because it enables a real articulating movement. However, from the perspective of small strains, both models exhibit a reasonable approximation. A unified phalanx for removing the cartilage between phalanges (single toe), which is frequently utilized by some authors [15, 85], is a more serious simplification. Some authors explain that the contact stresses applied to the forefoot do not flex the interphalangeal joints at a moderate velocity in a normal gait; therefore, significant inaccuracies in the predicted stress distributions are not expected [8]. This simplification is only suitable when the objective is kept away of the forefoot.

Regarding linear elastic properties, cartilage is defined as an incompressible material for an instantaneous response [86]; thus, a Poisson's ratio of 0.4 is common to the literature. The Young's modulus value is more controversial with two different values—1 and 10 MPa. The first value was derived in a study about cartilage biomechanical properties in the human cadaveric first metatarsophalangeal joint by Athanasiou et al. [87]. The value of 10 MPa was identified in previous literature based on the linear elastic properties of the knee FE model suggested by Schreppers et al. [88]. The selection of both values may be appropriate because higher values are frequently applied to larger joints, such as knee [89] and lower values are frequently applied to smaller joints, such as finger joints [78]. A value of 10 MPa may be more suitable for tarsus, whereas a value of 1 MPa may be suitable for phalanges.

3.2.2 Ligaments

Ligaments consist of the fibrous connective tissue that maintains contact with the bones across joints. They are a biological composite that consists of a ground substance

matrix reinforced by closely packed collagen and elastin fiber bundles. The ground substance matrix is composed of proteoglycans, glycolipids, fibroblasts and water [90]. Cartilage enables free slipping among bones, ligaments guide joints in a normal motion, which provides stability for the joints.

The main purpose of including ligaments in a foot model is to simulate the articulation function of providing guides to maintain touch with the head bones and provide stability for the hindfoot. For this purpose, ligaments in the foot simulation are represented by truss elements or springs. Both elements are one-dimensional and only support tensile forces, whereas the compression forces are withstood by cartilage. Thus, the difference between the options is that springs are independent of the cross-section and employ stiffness as the input property. An accurate geometry of the ligament is only used for studies of injuries to specific ligaments, such as the anterior cruciate ligament in the knee [91, 92]. The same situation applies to material properties. Despite the fact that ligaments exhibit a viscoelastic behavior [93, 94], a linear elastic approach is usually applied to ligaments in foot models, with the exception of special applications in which the ligaments are the focus [95]. These arrangements are distinct in the knee–ankle–foot model presented by Liu and Zhang [41], in which the knee ligaments were defined as hyperelastic properties with an accurate geometry and the foot and ankle ligaments were simulated as tension-only truss elements with linear elastic properties.

Due to the functional nature of these components in foot simulation, the literature contains minimal discussion on this topic. The majority of the models use a Young's modulus of 260 MPa and a Poisson's ratio of 0.4. These values were extracted from a study of the mechanical characteristics of the collateral ligaments of the human ankle joint by Siegler [96]. Due to advancements in computer science, recent models have begun to use nonlinear approaches for these applications [27, 97], which may provide insight on future foot models.

3.2.3 Tendon and Muscle

Tendon is the tissue that connects bone and muscles at their ends and transmits the forces generated by muscles to the bony structure. They have a multi-unit hierarchical structure that is composed of collagen molecules, fibrils, fiber bundles, fascicles and tendon units. These fiber bundles are aligned with the long axis of the tendon and provide the tendon's tensile strength. Tendons exhibit fiber patterns and viscoelastic characteristics; their typical stress–strain curve has an initial maximum strain of 2 % followed by a linear region until the ultimate strain with macroscopic failure [98]. Unlike muscle fibers, which exhibit passive

and active behaviors, tendon fibers only exhibit passive behaviors where the stress is dependent on the strain.

Within foot tendons, the Achilles tendon is the most important tendon because it is one of the strongest tendons in the human body; it bears enormous forces [99] and frequently fails by rupture [100]. Its importance is evidenced by the substantial amount of literature dedicated to this tendon compared with any other tendon in the lower limb. The majority of the properties of the remaining tendons of the foot are extrapolated from the Achilles tendon. The mechanical properties of the Achilles tendon have been examined in vivo [101–103], by the cadaveric tensile test [104, 105], and by the microtensile test [106]; the Young's modulus generally varies between 0.2 and 2 GPa. The information about other foot tendons is incomplete, the majority of the tests provide data on structural parameters, stiffness [107, 108] or cross-sectional areas [109–111] of different tendons. Few studies discuss the material properties of the extrinsic foot tendon [112–114], for which the data are similar.

Despite their analogous mechanical response to ligaments, which is dominated by the collagen fibers, the majority of the proposed models focus on predicting the ligament response; few simulations of foot tendons have been performed. In complete foot models, feeble attempts have been made in which tendons were simplified by truss/bar elements that approximate the actual tendon trajectory [29, 44, 115]. The tendon activity is only introduced in the model to directly transmit the forces to the bone insertions. A more accurate numerical approach was proposed by Gu et al. [116], who presented an incompressible, hyperelastic, two-parameter Mooney–Rivlin formulation to investigate the mechanical response of the Achilles tendon for different types of sports.

Few models have considered muscle tissue. The majority of the authors define a bulk fat connective tissue with weighted material properties, such as in trabecular and cortical bone. The 2D foot model proposed by Wu et al. [59, 70] distinguishes the passive properties of the muscle from the fat tissue. Note the study by Spyrou and his group [117], who defined a constitutive model for muscle–tendon coupled behavior with active and passive responses and his application to the simulation of human foot movements [118].

3.2.4 Plantar Fascia

Fascia is a type of tendon with a similar histologic but a flattened layer shape. Its main function is to join the muscles and the body parts that the muscles act upon. In particular, plantar fascia serves an important role in absorbing foot–ground impact, storing and returning strain

energy, transmitting Achilles tendon forces and maintaining arch stability [119–121].

Similar to ligaments, plantar fascia is modeled for its mechanical function in the foot structure to maintain stability in the medial longitudinal arch; however, its morphology and mechanical behavior is not refined. Plantar aponeurosis is only modeled when the entire foot is involved and is neglected in partial geometry models. It is typically simulated with truss elements—one per ray—that join the calcaneal tuberosity with the base of each proximal phalange [122, 123]. The properties applied to these tension-only elements are usually linear elastic models with a Young's modulus of 350 MPa and a Poisson's ratio of 0.4. These parameters are based on the experimental test of the elastic properties of plantar fascia, which was performed by Wright and Rennels [124]. Because of the important role of plantar fascia in human locomotion, some authors employed more accurate nonlinear approaches [24, 27]. The data for adjusting the terms of the functions were obtained from clinical research results [125].

Recent investigations have expanded the nonlinear mechanical properties of this tissue as a basis to develop suitable numerical models [126, 127]. A dynamic simulation of the plantar fascia during the entire stance phase of a gait has been performed using transversely isotropic properties [40]. Those approaches comprise an important step for future simulation.

3.2.5 Fat and Skin

In foot modeling, fat tissue is referred to as the fat pad; it is located under the calcaneal and metatarsal heads. However, fat tissue is also located in other parts of the foot. For mechanical purposes, the properties of the fat pad are considered. This tissue is commonly referred to as plantar soft tissue. The heel pad is a highly specialized structure that is designed to resist compressive loads; it consists of packed fat cells that are enclosed by elastic fibrous connective tissue [128]. This soft tissue is characterized by nonlinear and time-dependent behaviors, that is, the level and the rate at which the tissue is loaded influence its instantaneous stiffness [129].

This viscoelastic tissue provokes substantial interest in the development of a more refined characterization of its mechanical properties due to its strong relationship with diabetic ulcerations and the complexity of measuring its internal stresses. In this regard, many numerical approaches have been provided based on *in vivo* and *ex vivo* test data: the viscoelastic Voigt–Kelvin model [130], the hyperelastic Mooney–Rivlin model [129, 131], the hyperelastic first-order Ogden model [132, 133], the quasi-

linear viscoelastic theory [134] and the visco-hyperelastic formulation [135]. These approaches were based on the stress–strain curve under compressive load of the heel pad, with the exception of the fitting of coefficients provided by Ledoux & Blevins [134], which were adapted from stress relaxation experiments of six different regions of the plantar soft tissue.

These approaches have not been run in 3D complete foot FE applications. Viscoelastic formulations have only been applied in partial geometrical models [17, 45, 136]. In complete 3D foot simulations, a hyperelastic formulation is applied to an encapsulated bulk soft tissue, in which the skeleton is embedded. This volume includes fatty tissue, muscles, tendons and the skin layer; it is frequently characterized with the parameters calculated by Lemmon et al. [7] and Erdermir et al. [132]. For simplicity and to reduce the computational cost, this bulk tissue was also assumed to be linear elastic [137–139]. The most detailed representation of heel pad geometry was the FE model that considered fat cells and their septa fiber structure; they were modeled separately using different material properties [140].

In the last few years, numerical models have been gradually developed to separately simulate skin behavior from fatty tissue behavior. These studies primarily focused on the influence of this fibrous tissue on the internal stress of the fat pad. The hyperelastic Ogden formulation was initially proposed to describe skin behavior [141, 142]. A recent approach based on a fiber-reinforced hyperelastic model has been provided by the research group led by Natali at the University of Padova [23, 143]. In their latest study, they analyzed the mechanics of foot skin with a special focus on the orientation and distribution of the fibers that characterize the anisotropic response of the skin [144].

4 Foot Model Applications

FE foot models provide a vast amount of data, which can be useful in different fields. These applications can be grouped into two main areas: (1) biological and clinical applications and (2) orthosis and footwear design. The former includes physiological analysis, pathological and foot disorder studies and surgical and healing treatment evaluations. The latter involves the design and optimization of orthotic devices, shoe soles and other shoe components. In this section, existing studies are sorted and exposed in a compressive manner to demonstrate the extensive range of studies that have been performed with FE foot models. The type of model and the validation method are discussed.

4.1 Clinical Applications

Some recurrent topics in clinical applications are as follows: the study of the stress distribution in a gait, the relevance of each structure in the foot arch function, ankle ligaments injuries, car crash impacts, the plantar stress distribution on the diabetic foot, hallux pathologies, plantar fasciitis surgery and the comparison of different procedures for claw toe. Computer foot models that consider partial, total, simplified or geometrically detailed foot structures, which were intended for clinical applications, are reviewed.

4.1.1 Physiological Studies

Because direct measurements of the stress distribution within the human foot *in vivo* are not feasible, the use of models became necessary. First, studies that discussed and proved the potential of the FE method in the simulation of the mechanical behavior of the human foot are presented.

In 1993, the medial arch of a human foot was modeled to investigate the internal stress pattern. The 2D single bone model presented by Patil et al. [145, 146] was intended to calculate the physiological state as a reference to examine and improve the comprehension of foot disorders. The same authors subsequently performed a similar study with an oversimplified 3D two-arch model of a normal foot [147]. With a similar purpose, Andrea et al. [148] explored the strain distribution of the calcaneus in a 2D sagittal view as guidance for more complex models. Unlike the bony model presented by Patil et al., Andrea et al. included nonlinear properties of the soft tissue. Calcaneal loading was also assessed by Gidding et al. [149] for walking and running conditions. Their scalable subject-specific calcaneus/foot 2D model was capable of predicting normalized peak forces for the Achilles tendon, plantar fascia and plantar ligament, which exhibited quantitative agreement with the *in vivo* measurements.

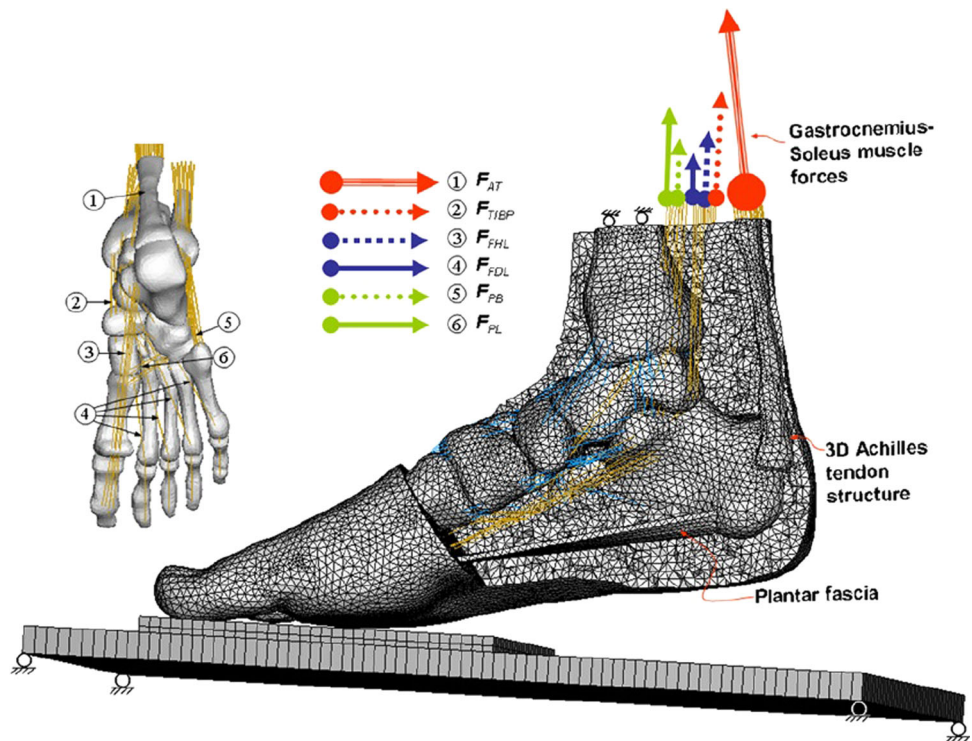
Consistent with understanding the biomechanics associated with the normal foot, Chen et al. [13] established a preliminary 3D FE model to estimate the stress distribution in the foot from the midstance phase to the push-off phase in a barefoot gait. To simulate the relative movement of the floor with respect to the foot, they constructed a rigid plane to apply a constant linear velocity and an angular velocity that moves toward the foot. Using this floor movement and by immobilizing the upper tibial nodes, they set the loading and boundary conditions from the midstance phase to the push-off phase. A similar objective was achieved by Gefen et al. in a different manner [8]. They analyzed the biomechanics of the foot structure in discrete events during the stance phase of a gait. They performed an experimental analysis to gather information about both the kinematic and

dynamic forces of the foot in a gait, which helped to define the boundary conditions in all phases of a gait by trial and error. Their 3D model considered the nonlinear behavior of the soft tissue. The objective of these studies was to define the stress reference state (baseline case) of the normal foot for both pattern (qualitative) and range (quantitative), which facilitates the identification of highly elevated stresses when compared with a pathological foot.

After a significant improvement in computational power and tools, geometrically detailed models for exploring the role of the main lower leg muscles in a human gait were developed. In particular, Takahashi et al. [138] investigated the importance of considering the spontaneous plantar flexion of a gait. They performed an experimental measurement of the motion, the reaction force and the contact area of the human foot. Information about the position of the ankle and the displacement of the heel for simulating the Achilles tendon force was given as boundary conditions in their 3D FE foot model. Chen et al. [44] analyzed the contribution of the gastrocnemius–soleus and other plantar flexor muscles during heel rise. This analysis was performed using a sophisticated FE musculoskeletal model with hyperelastic material properties and real Achilles tendon geometry, as shown in Fig. 5. The values of the muscle forces and local plantar pressure peaks were compared with *in vivo* experiments, and strains in the second metatarsal were compared with the cadaveric measurements. Another model that addresses the high degree of complexity of the musculoskeletal system of the human foot was proposed by Qian et al. [29]. A 3D FE foot model that comprises 29 bones, 85 ligaments and the plantar soft tissues was used to study the foot arch and plantar fascia deformations in the midstance phase. In this model, only muscle forces and ankle joint forces acting on the talus bone were utilized to drive the model. A subsequent study that employs this model and a FE heel pad model, which consists of fat cells and a reticular fiber structure, was introduced with the biological coupling theory [140]. They examined the biomechanical response of the coupling mechanism of the heel pad (impact attenuation function) and the foot arch (energy absorption function). They suggested that the impact attenuation and energy absorption function of the foot is the coupling result of both subsystems. The muscle-driven simulation was also applied by Spyrou and Aravas [118]. They described a FE scheme for realistic muscle-driven simulation of human foot movements. Their lower leg model was used to estimate internal stresses and strains and shape changes of the deformed tissues during plantar flexion of the ankle.

The dynamic foot response over the entire stance phase was analyzed by Qian et al. [150]. A 2D subject-specific dynamic FE foot model was developed and validated with gait measurements. A sensitivity analysis of the material

Fig. 5 Complete foot FE model including muscle forces with real geometry of Achilles tendon and plantar fascia [44]



properties and frictional and damping coefficients was also performed. They suggested the use of dynamic analysis over the quasi-static step analysis to simulate dynamic motions. The greatest challenge in dynamic studies is the computational time. With the intention of reducing the computational cost, Halloran et al. [151] presented a musculoskeletal model coupled to a FE model of the foot using an adaptive surrogate modeling scheme. The FE model and the musculoskeletal model were directly coupled by sharing boundary conditions at a point in the talocrural joint. With this technique, they were able to study the peak pressure and ankle vertical load as a function of time for the optimal solution to maximum height jumping. In a subsequent study with the same procedure, they predicted a substantial reduction in peak strain energy density in plantar tissue under metatarsal heads, which alters gait patterns [152]. Chen et al. [136] also employed the technique of combining two models to perform a dynamic study. In this case, a visco-hyperelastic heel and shoe FE model was combined with a spring-dumper-body model to analyze the heel/shoe dynamics during running.

In addition to a gait analysis, the foot arch stability and windlass mechanism of the Achilles tendon is a frequent topic in the literature. A computational study by Cheung et al. [153] explored the relationship between plantar fascia and the Achilles tendon; they determined that an increase in the Achilles tendon load resulted in a reduced arch height and increases in plantar fascia stresses. They also present the fascia as an important arch-supporting

structure. This idea was expanded by Wu [70], who demonstrated that plantar longitudinal arch function is supported not only by plantar fascia and ligaments but also by intrinsic muscles. The FE estimations were validated with plantar pressure measurements, electromyography activity and anatomical experiments. The connection between plantar fascia strain and the Achilles tendon force, which is known as the windlass mechanism, was also computationally simulated by Cheng et al. [24]. Their results corresponded with the results of previous studies, which indicated that the plantar fascia strain increased as the dorsiflexion and Achilles tendon force increased. The fascia stress underneath the first foot ray gradually decreased as it moved toward the fifth foot ray. Recently, Lin et al. [40] developed a 3D dynamic foot model to estimate the stresses in the plantar fascia during the entire stance phase. Kinematic data and ground reaction forces were measured from a healthy subject to validate the model. Sun et al. [139] analyzed the relationship between different foot arches and stress variations inside the foot. From a standard FE foot model, four models were generated, in which the original arch height varied from a low-arched configuration to a high-arched configuration. In the low-arched foot, high stresses were detected in the rear and midbones, whereas high stresses in the forefoot and fascia were detected in the high-arched foot. The predicted strains and stresses in these studies contributed to an enhanced understanding of the complex foot arch function and may have practical implications in plantar fascia and ligament release interventions.

4.1.2 Injuries

For clinicians, understanding the risk of foot injury due to mechanical loading is essential. Biomechanical measurements can provide important information about the total reaction forces but cannot directly assess the internal stress state of the foot. In these cases, the FE method becomes a very useful tool, which can be used to better understand the mechanical responses of biological systems. This information is valuable not only for clinicians but also for other professionals. For example, in the area of car crash injury, a better understanding of injury mechanisms helps in the design of safety devices. In this context, the study by Beaugonin et al. [154, 155] was framed. The model was initially validated against inversion/eversion and dorsiflexion responses and subsequently applied by Kitagawa et al. [156] to study tibial pylon fractures in frontal crashes. They studied the combined effect of muscle preloading and external force by applying the Achilles tendon force to the calcaneus while an external impact force was applied to the forefoot. The results were compared with the results from the dynamic impact test in cadaveric specimens. This model was subsequently revised to examine the dynamic response after adding plantar aponeurosis and modeling metatarsal joints [157]. Ankle skeletal injury under high-energy compressive force was evaluated by Iwamoto et al. [158]. They implemented an anisotropic inelastic constitutive model of cortical bone by considering damage evolution in a lower limb FE model. A parametric study on ankle skeletal injury was performed in terms of footwell intrusion and pedal impact. Beillas et al. [159], who specifically noted the importance of properly setting (stiffness and position) the ligaments and fat pad, presented a baseline model to investigate car crash injury.

The injury tolerance of the ankle ligaments were examined by Shin et al. [47]. They developed a complete foot and leg FE model to analyze the failure of the ligaments and focused on a range of experimental forces in vehicle crashes. Several simulations for different loading conditions, including forefoot impact, axial rotation, dorsiflexion, and combined loadings, were performed based on previous tests to validate the model. Internal and external ankle rotated postures under brake pedal loading were simulated. Ligament failures were predicted as the main source of injury. Regarding ankle ligament injury, some models were specifically developed and validated with experimental cadaver studies. Such as the case of the computational model developed by Liacouras et al. [160] to assess syndesmotic injury and ankle inversion stability. In addition, the model was also capable of predicting joint kinematics, which were not easily obtained via experiments. The focus of this study was the changes in joint function after repair of a syndesmotic injury by insertion of

a fracture staple and the increase in force experienced by other ligaments after transection of the calcaneofibular ligament. Similarly, Liu et al. [161] evaluated the treatment of inferior tibiofibular syndesmosis injury using a transverse syndesmotic screw. Although that treatment effectively stabilizes syndesmotic diastasis, it decreases the joint's range of motion, and therefore, fixation should not be performed for an extended period of time. Wei et al. [162, 163] measured the normal dorsiflexion, eversion, and external rotation of some subjects to drive a 3D multibody computational ankle model, which was employed to study the mechanism of high ankle sprain. The model predicted the strain of the anterior tibiofibular ligament in the motion sequence and a peak strain in the anterior deltoid ligament, which parallel the cadaver studies. They suggested that the posterior talofibular ligament injury caused by excessive levels of external foot rotation is a function of foot constraint and proposed additional studies to design shoes to minimize the injury risk.

Tannous et al. [46] presented a preliminary study that characterized the foot–ankle complex for axial impact loadings by calibrating it against data tests. This model was used as a basis for developing a 3D lower limb model to investigate impact injury [12]. To evaluate the model, they conducted a series of experiments on the impact of a pendulum on a cadaveric lower extremity at various initial velocities. The results indicate that the calcaneus, the tibia and the talus experience the largest amounts of stress. Significant stress was detected in the lateral-collateral ligaments. Instead of ankle ligament injuries, the simulation performed by Gu et al. [164] changed the study focus to metatarsal injuries for landing impact. The deformation and stresses in the metatarsals at different inversion landing angles were comparatively evaluated. The results showed that stresses increased in the lateral metatarsals, whereas stresses decreased in the medial metatarsals with increasing inversion angles. It was found that the stiffness of the slip fascia is an important factor in the fifth metatarsal fracture. The stresses in the deep heel (calcaneal tuberosity) during walking were estimated by Spears et al. [165]. They suggested that the plantar heel pain is generally higher when the heel is loaded in an inclined position. Peak internal compressive stresses were larger than the external plantar pressure. This estimation was calculated with a lower heel FE model with viscoelastic behavior and validated in vivo against mean and peak external plantar pressures. A different visco-hyperelastic constitutive model was formulated by Fontanella et al. [23] to simulate the mechanical response of the heel tissues for different strain rates. Their 3D subject-specific heel pad model also included a fiber-reinforced hyperelastic formulation for the skin, which was a limitation of the Spears' model. Stresses in this region were also dynamically analyzed by Qian et al. [140] during

barefoot walking and by Chen et al. [136] during shod running as previously mentioned.

4.1.3 Pathomechanics

A reasonable understanding of feet pathologies and disorders is crucial to determining the best treatment. The plantar stress distribution of a diabetic foot has been extensively and computationally investigated. Patil et al. [6] simulated muscle paralysis from accidents or diseases such as leprosy or diabetes and its effect on the distribution of principal stresses. A 2D FE model was used to analyze three quasi-static walking phases. The results demonstrated that both the shape of the foot and the type of muscle paralysis contribute to the development of large stresses in different regions of the foot, which may be an important factor in the process of tarsal disintegration in leprosy. A similar study with a 3D two-arch model of muscle paralysis, which is associated with Hansen's diseases, was accomplished [11]. Their model predicted areas of the bone that disintegrated due to decreased mechanical strength of the bone in this region. This model was subsequently improved and characterized in a push-off position and performed to evaluate the effect of foot sole stresses on plantar ulcer development [83] by simulating three decreasing thicknesses of foot sole soft tissue in the forefoot region with increasing hardness. FE analyses for the diabetic subject foot models showed that the normal and shear stresses at the foot sole-ground interface increased compared with corresponding values for the control subject with increased hardness and decreased thickness in the foot sole soft tissue in the forefoot region. The authors suggested that these high stresses in the foot soft tissue might be responsible for the development of plantar ulcers in diabetic subjects. This idea was also supported by Gefen [10]. His results suggested that the process of injury in diabetic feet is likely to initiate in deeper tissue layers especially in the plantar pad underlying the metatarsal heads. The model comprised five planar longitudinal cross-sections through the foot. The total load and muscle forces were distributed by weight in the first ray through the fifth ray 2D models. The same hypothesis was analyzed in another study [166]. The results confirmed the clinical findings: bony prominences, such as the metatarsal heads, served as stress risers. In subsequent years Chen et al. [22, 167] also computationally analyzed this feature of the disease. Their 3D foot model indicated that large stresses occur where plantar soft tissue contacts geometrically irregular bony structures. Thus, the internal stress distribution within the plantar soft tissue was significantly influenced by bony prominences due to the stress concentration, as shown in Fig. 6. The subject-specific model was validated by comparing the experimental measurements of

the plantar pressure distribution and internal plantar tissue deformation. The idea that the internal stress is higher than the surface pressure was explored by Fernandez et al. [168]. They developed an anatomically-based subject-specific foot model that separately considered muscles, bones and soft tissue layers. Using anisotropic properties, they detected maximum internal stress values that were 1.6 times higher than the surface pressure values, which is consistent with the hypothesis that injuries may initiate in the deep tissue structures and may not be detected during a clinical evaluation.

The effect of the increasing severity of diabetes was investigated by Cheung et al. [15]. They simulated the increasing stages of diabetic neuropathy, in which the soft tissue stiffness increases by 2–5 times the normal values. The 3D foot model predicted an increase in peak pressure in the forefoot, midfoot and rearfoot regions and a decrease in the contact area between the plantar foot and the support in the entire foot, which caused an increase in the gravity of the disease (increased soft tissue stiffening). The relationship between soft tissue stiffness and ulceration was also analyzed by Sopher et al. [17] with a focus on the heel region. The risk of heel ulceration associated with foot posture during bedrest was investigated. Based on the results of the posterior heel FE model, a higher risk of heel ulceration was discovered for abducted foot posture compared with upright foot posture. With regard to foot posture, Brilakis et al. [137] analyzed the effect of foot posture on fifth metatarsal fracture healing. Thirty 3D FE models were compared by considering fracture type, foot posture, and healing stage. No statistically significant differences were observed for different foot postures. An ulcer formulation was constructed to better understand the biochemo-mechanical process of foot ulceration and its progression. In this first step, a two-phase model of soft plantar tissue was applied to a 2D foot FE model to simulate several gait cycles of a healthy foot [169].

In addition to leprosy and diabetes, other pathologies have also been examined. Budhabhatti et al. [25] presented a realistic FE model of the first ray used to perform a kinematical study of the late-stance phase of walking. This study focused on plantar pressures underneath the first ray in three different cases: pathology (hallux limitus), surgery (arthrodesis), and conservatory treatment (therapeutic footwear). A metatarsophalangeal joint FE model was also employed by Flavin et al. [21] to challenge the many etiological theories of hallux rigidus. They postulated an increase in stress of the plantar fascia as the cause of abnormal stress on the articular cartilage instead of a mismatch of the articular surfaces or subclinical muscle contractures. This finding may influence the treatment of early stages of hallux rigidus. Tao et al. [84] investigated the relationship between hallux valgus and hypermobility

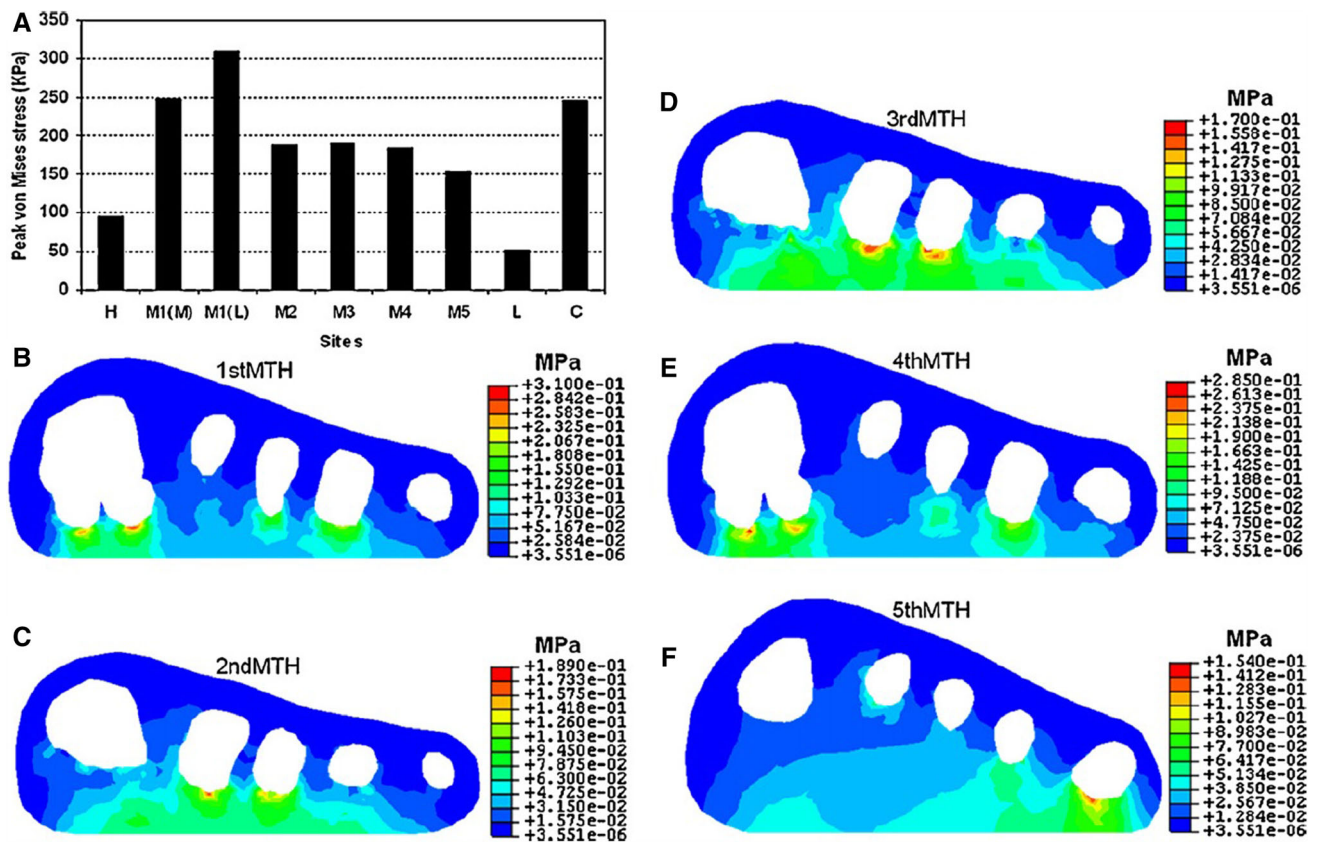


Fig. 6 Internal von Mises stress of plantar soft tissue under each metatarsal head [22]

of the first metatarsocuneiform joint. Their skeleton FE foot model predicted the plantar and medial displacement of the first metatarsal, which can affect the normal function of the first ray under repeated weight loading of the gait cycle. The same hypothesis was used in a computational study with a more detailed model [170]. The joint forces at the metatarsocuneiform and metatarsophalangeal joints of two FE foot models (a normal foot and a foot with a hypermobile first ray) were compared. The results suggested that the hypermobility of the first ray increased the loading of both joints and caused them to be predisposed to the risk of joint problems.

4.1.4 Surgical Treatments

The experimental verification of clinical procedures is frequently lacking. As a supporting tool in experimental cadaveric studies, computational modeling approaches can provide the means to explore different interventional procedures. As in product design, in which the product is modeled after initial trials to save money and time spent on prototyping, these approaches are also applicable in clinical procedures. Surgical interventions can be simulated as a step toward additional analysis to reduce the number of

trials required to obtain an effective procedure and to shed light on pre- and post-surgery evaluations that are frequently difficult to quantify.

Several studies about plantar fascia release intervention have been published. This treatment was initially modeled by Gefen et al. [171]. Their five rays FE model estimated a large sagging of the arch and a significant increase in the long plantar ligament. These results were similar to the results of a subsequent study, in which the authors applied more accurate material properties in the model and suggested that surgery may reduce the dynamic shock-absorbing abilities of the foot and cause additional musculoskeletal damage [9]. This finding is consistent with the predictions of a 3D foot model performed by Cheung et al. [14]. In their study, the biomechanical responses of the ankle-foot complex with different plantar fascia stiffness were quantified. The results indicated that significant stresses are induced in the ligamentous and bony structures when plantar fascia stiffness decreases; non-operative treatment was recommended. In the case of surgery intervention, a partial release of less than 40 % of the fascia was recommended to minimize the effect on arch instability [172]. This recommendation was also suggested by Liang et al. [43]; their 3D foot model did not predict total collapse

of the foot arch until all four major plantar ligaments were simultaneously sectioned. Unlike the previously mentioned models that validated and compared predictions with plantar pressure distributions and radiologic measurements, Liang and coauthors tested seven fresh adult cadaveric feet to measure the displacement of the four major bone segments and stabilizers of the foot arch and to compare with the FE results. Similarly, Tao et al. [173] simulated four cases after individual release of the plantar fascia and three major ankle ligaments. Although arch collapse was not predicted after each structure sectioning, a significant increase in tension in the remaining ligaments was predicted. According to these studies, the model proposed by Iaquino et al. [174] predicted high strains after plantar fasciotomy and identified plantar fascia as the greatest contributor to arch stability.

Several FE studies have been performed to investigate the biomechanics of toe interventions, that is, the previously mentioned first toe models of Budhabhatti et al. [25] and Flavin et al. [21]. The first study defined different dorsiflexion fixation angles and compared them with conventional angles to reduce plantar pressures in first ray arthrodesis surgery. Flavin et al. addressed the surgical procedure for the treatment of early stages of hallux rigidus. Osteotomy in the first ray for correction of hallux valgus deformity was analyzed by Matzaroglou et al. [175]. Unlike the majority of computational studies, this simulation was performed to confirm the positive long-term clinical results of the 90° Chevron osteotomy.

Other toe surgeries that were computationally evaluated entailed the correction of claw toe. Studies by Garcia-Gonzalez et al. [26] and Bayod et al. [115, 176] presented an alternative technique to the proximal interphalangeal joint arthrodesis for the correction of hammer toe and claw toe deformities. They compared the effectiveness and risks of two recent techniques against the traditional procedure in a complete foot skeleton FE model in the push-off position. Similarly, Isvilanonda et al. [27] compared the modified Jones procedure with the Flexor Hallucis Longus tendon transfer for the correction of clawed hallux deformity and determined that the most suitable procedure varies depending on the presence or absence of Flexor Hallucis Longus overpull.

FE simulations not only aid in the evaluation of clinical procedures but also quantitatively define guidelines for surgical treatment. For example, Bayod et al. [20] estimated 1.30 cm³ as the maximum of harvested calcaneus to prevent the risk of calcaneus fracture after surgery. The estimation was based on a series of calculus where the depth of bone excision and the Achilles tendon force gradually increase, as shown in Fig. 7. A previously mentioned study recommended a maximum of 40 % of plantar fascia release to minimize the arch instability [172].

The post-surgical effects of tarsometatarsal joint fusion was evaluated by simulating a normal foot and an operated foot [177]. The results that were validated with plantar pressure distribution during three instants of gait showed an increase in the stresses in the second metatarsal bone, which made it susceptible to fracture. Garcia-Aznar et al. [69] developed a 3D foot skeleton model to evaluate the stress distribution of four different metatarsal configurations, which helped physicians to perform metatarsal osteotomies to adjust the incorrect geometry of the metatarsal bones. Trabelsi et al. [51] focused their study on the fracture of metatarsal bones to investigate the influence of a distally located drilled hole in the second metatarsal bones, which is a common Hallux Valgus surgical correction procedure. The single metatarsal bone model predictions were validated on a large number of experiments performed on metatarsals bones from different donors.

4.2 Orthosis and Footwear Design

Orthosis design, material and shape, have been extensively explored by FE method as alternative treatments for many foot pathologies; they are preferred to invasive methods such as surgery. The parameters for footwear design are of significant interest to the footwear industry. There is an extensive range of applications, including therapeutic orthosis, insole design, sport footwear, military boots and high-heeled shoes, focus on reducing plantar pressure because pressure on the plantar foot has been associated with perceived comfort and pain generation [178, 179].

4.2.1 Therapeutic Orthosis

Diabetic and Hansen's disease patients are frequently prescribed therapeutic orthosis to relieve elevated plantar pressure and to prevent plantar ulceration. The design of these types of orthosis is based on the experience of the practitioner and adheres to a trial and error process. Numerous studies were conducted to help researchers design optimal orthosis for a desirable plantar pressure distribution.

To reduce plantar pressure, some authors focus their research on material properties of the therapeutic orthosis. Despite its limitations, the pioneer FE analysis presented by Nakamura et al. [5], established the basis of posterior studies. Their 2D idealized foot was designed to estimate the range of elastic properties of the shoe sole that minimized peak stresses within the soft tissue. They performed a simple material test to define nonlinear behavior of the heel soft tissue and a convergence study to establish the method of calculus. Lemmon et al. [7] also performed a uniaxial in vivo test of the heel soft tissue. Data on five subjects were collected using an ultrasound device to

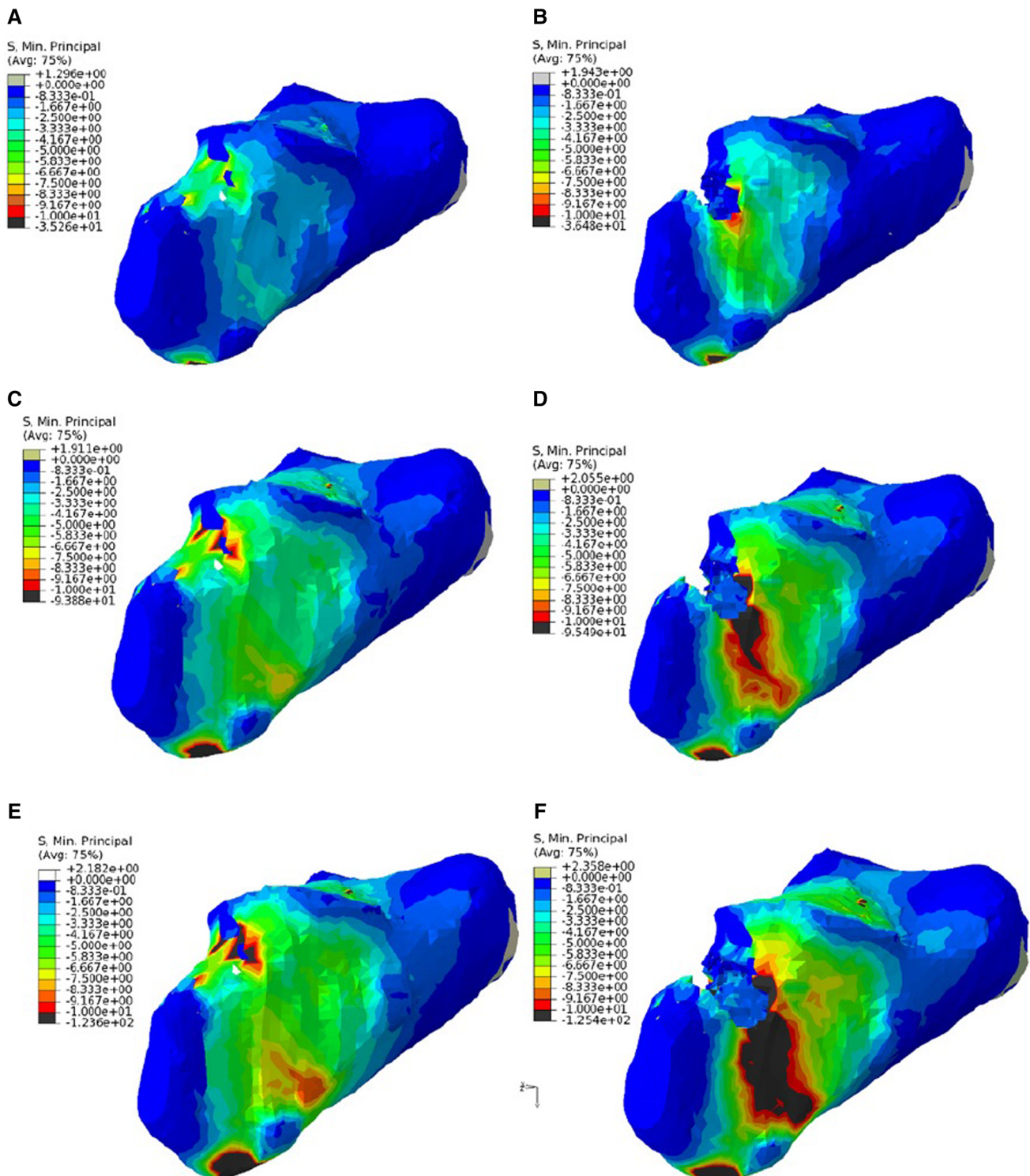


Fig. 7 Compression stress in the calcaneus increasing gradually size of bone excision and Achilles tendon force [20]

measure tissue displacement and a load cell to measure force. The data were introduced in a 2D second metatarsal head model to investigate alterations in pressure under the metatarsal head as a function of insole and tissue thickness. The results predicted that peak pressure in the soft tissue

decreases as the insole thickness increases; this effect intensifies with thin soft tissue. Erdemir et al. [180] also presented a 2D FE model of the second metatarsal bone to analysis plugs located in the midsole. Thirty-six plug designs were investigated: a combination of three materials,

six geometries, and two placements. The results suggested that the placement of plugs based on plantar pressure measurements are more effective for reducing peak plantar pressure. A similar study was performed by Actis et al. [181]. With a 2D second ray FE model, several design variations were examined, with variations such as changes in the number of plugs, plug diameter, distance between plugs, plug height and material properties located in the insole under the metatarsal head. The results demonstrated that customized inserts with softer plugs distributed throughout the regions of high plantar pressure are more effective for decreasing peak plantar pressure than total contact inserts. Unlike these studies, which were focused on the stresses under the metatarsal heads using 2D sagittal models, Gu et al. [182] investigated the properties of the midsole plugs under the calcaneus with a 3D complete foot model. The effect of material properties and the thicknesses and dimensions of the plugs on the plantar pressure distribution during the heel strike phase was systematically analyzed to optimize the design. Another study that evaluates the influence of different material characteristics on the mechanical response of the heel pad region was the computational analysis by Fontanella et al. [183]. A 3D heel FE model with linear orthotropic formulation for bone, visco-hyperelastic formulation for fat, fiber-reinforced hyperelastic formulation for skin and hyperfoam formulation for insole was employed. Different combinations of materials for midsole and insole layers were considered to evaluate the mechanical behaviors of the heel pad tissues at the heel strike in bare and shod conditions.

Other authors, such as Chen et al. [73], assessed the reduction in peak plantar pressure via stress redistribution using total contact insoles. The results of their FE analysis of total contact insoles against flat insoles showed that the total contact insole redistributes the stresses and decreases the peak pressure in the heel and metatarsal regions. A similar study by Lin et al. [184] obtained the same conclusion. Total contact insole can significantly offer pressure relief compared with flat insoles in forefoot and rearfoot regions. Lin & colleagues also measured this distinction in experimental tests. Consistent with these results, Cheung et al. [72] specifically focused their investigation on the effect of the custom-modeled shape vs stiffness of the material insole for peak plantar pressure reduction. The 3D FE analysis indicated that the insole's custom-molded shape is more important for reducing peak plantar pressure than the stiffness of the material from which it is constructed.

Liu and Zhang [41] recently developed a 3D FE model of the human knee–ankle–foot complex with orthosis to investigate the effect of lateral wedged insoles on the internal loading distributions in the knee joint, as shown in Fig. 8. The results of this lower extremity model suggest

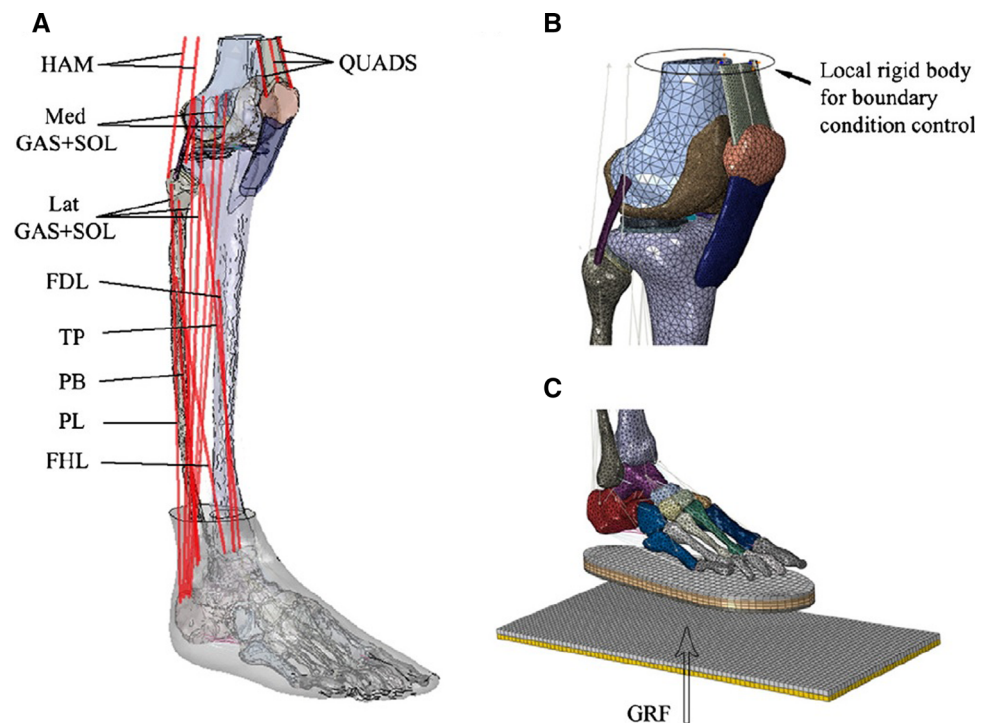
that the lateral wedged insoles can redistribute the knee internal loadings and relieve stress at the medial compartment of the knee. Other types of therapeutic orthosis have also been examined. A simple 3D model of a foot coupled with ankle foot orthosis was developed by Chu et al. [185]. This early 3D model was intended to confirm the peak stress position in ankle foot orthosis. They concluded that the stress distribution in the orthosis is dependent on patient body build and is distinctly asymmetric. They also confirmed the hypothesis that high stress concentration occurs in the neck and heel regions of the ankle foot orthosis, which is a common fracture point [186].

4.2.2 Insole Design Parameters

Therapeutic footwear has been proven to be effective in plantar pressure relief. Goske et al. [187] focused their research on the parameters of insole design. A plane strain heel-pad FE model was created to investigate the effect of three insole design variables (conformity, thickness, and material). The comparison of the 27 designs (combination of three levels for each variable) indicated that the full-conforming insole design provided the greatest reduction in heel pressure, whereas material selection had a minimal effect. A sensitivity analysis of five design factors of foot orthosis was subsequently performed by Cheung and Zhang [188]. Their statistics-based FE analysis revealed arch-conforming foot orthosis and softer insole material as the most important factors for peak pressure reduction. Other design factors, such as insole and midsole thickness and midsole stiffness, served less important roles. To assess these effects, FE foot models with 16 different orthosis configurations were constructed. Regarding the insole shape, Hsu et al. [123] implemented an optimization analysis to determine the optimal insole that minimized the junction stress between the plantar fascia and the calcaneus. They defined the von Mises stresses between the plantar fascia and the calcaneus as the objective function. The optimal resulting insole did not make complete contact with the foot plantar surface compared with the total contact insoles that were previously proposed. The symmetric heel FE model presented by Luo et al. [189] was developed to compute the stresses on the surface and within the plantar soft tissue under the calcaneus. They concluded that, the peak pressure near the calcaneus and on the skin surface should be reduced in the design of optimal insoles. These four cited studies were validated by comparing the plantar pressure predicted by the FE analysis with the plantar pressure measurements of the volunteers.

FE models of foot and footwear was also developed to evaluate the design of the soles. Using reverse engineering to construct the actual rocker sole, Lin et al. [190]

Fig. 8 FE model of the human lower limb to investigate the effects of wedged insoles in femur cartilage and meniscus [41]



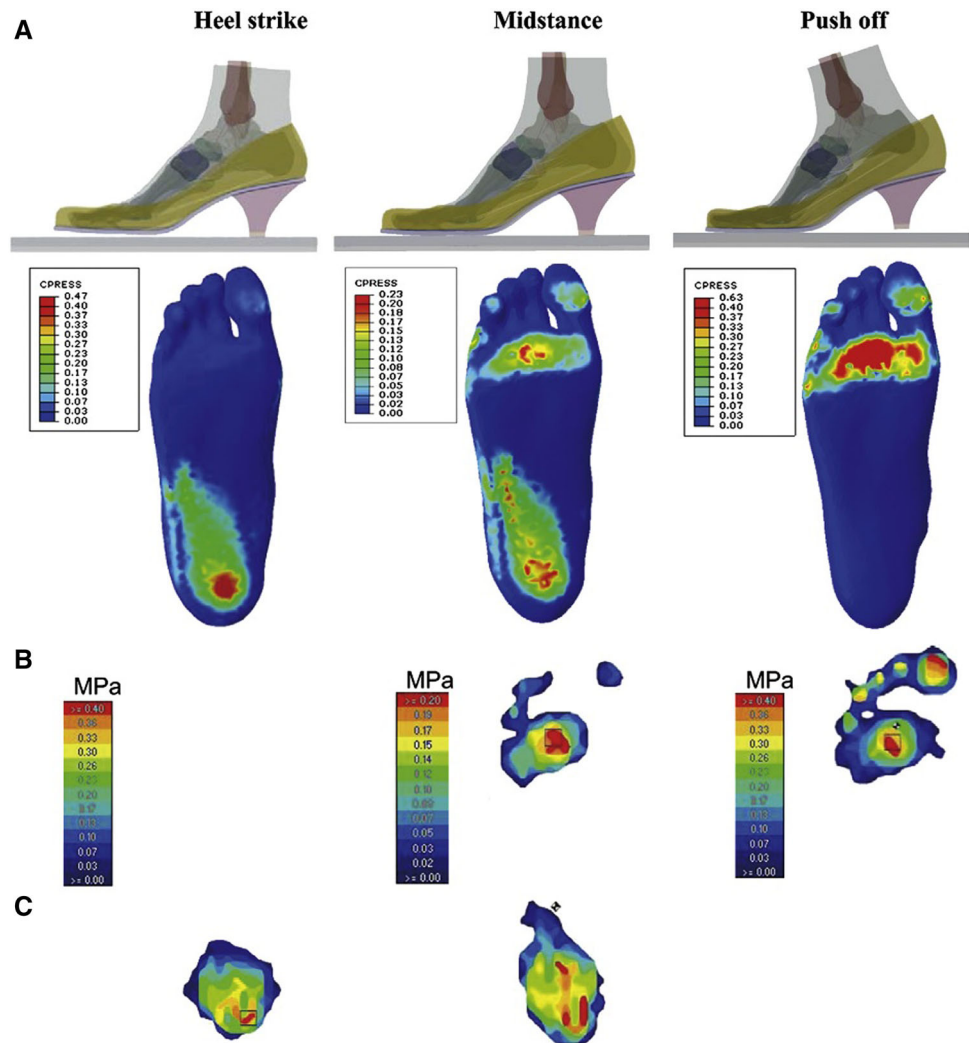
estimated the effectiveness of the sole design by dispersing the high pressure from the rearfoot and the forefoot to the arch region of the foot. These simulations are very useful for footwear companies, which can assess the biomechanical effect of their products without prefabricating samples and repeating subject trials. A review of footwear models for industrial applications was presented by Cheung et al. [191]. They summarized in a table the FE software, the geometry and number of elements, the material properties and boundary conditions, the parameters of interest and the type of validation process in numerous FE models that were published in the scientific literature until 2008.

4.2.3 Footwear for Impact Attenuation

Another interesting area in which FE models have been employed is the analysis of foot impact attenuation caused by the heel and the shoe for different activities. The most common impact on the human foot occurs during running. Verdejo et al. [192] conducted a study to evaluate the fatigue of the foam used in running-shoes midsoles and the possible cause of running injuries. They developed a 2D heel/shoe model to analyze the synergy response. Both materials were simulated with Ogden hyperelastic properties. Pressure distribution experiments on runners were performed to validate the analysis and to monitor changes in shoe cushioning. The peak plantar pressure was doubled after a 500 km run. A similar study also analyzed this

overuse of sport shoe foam. Even-Tzur et al. [193] used a lumped system and FE models to evaluate heel pad stresses and strains during running. In this case, a 3D half heel model considered the viscoelastic behavior of the heel pad and foam. The results showed that peak heel pad stresses were more sensitive to loss of foam thickness than to degradation in its viscoelastic properties. Peak heel pad stresses were consistently lower for running with shoes versus bare feet, even when properties of the foam were degraded. Cho et al. [194] introduced a 3D foot–shoe FE to evaluate the requirements of court sports shoes. They described the problem as the landing impact attenuation that accompanies every sport. The proposed model involved a detailed footwear simulation with complete contact interaction between the internal face of the shoe and the foot, at the expense of disregarding the majority of the singularities of the complex internal structure of the foot. These two independent meshes facilitated the individual prediction of the dynamic response of the foot and the sport shoe. The same concept was presented by Qiu et al. [16]. They developed a 3D coupled foot–boot FE model that focused on parachute landing impact; however, this model requires complete validation under static and dynamic loading conditions. The combination of the five rays as a whole for the sake of simplification was applied by Dai et al. [195] to investigate the effect of socks during walking. A foot–sock–insole contact FE model was employed to perform three dynamic simulations: a barefoot condition and two sock-

Fig. 9 Plantar pressure distribution predicted and measured from a female wearing high-heeled shoes [42]



wearing conditions. They concluded that shear force can be reduced by wearing the sock due to low friction against the foot skin and high friction against the insole compared with the opposite combination. This simplification of the foot as a whole without any detail of its inner structure has also been applied in other simulations with a highly demanding interaction of the outer layer, such as kicking a ball [48] or walking on mud substrate [196].

To investigate the effect of the confinement of the heel on internal fat pad stress, Spears et al. [141] performed a 2D FE model of the heel pad using either homogeneous or composite material properties (fat pad and skin). Based on the results, they suggested that the external confinement due to the heel counter of the shoe functions similar to skin walls by providing external pressure to the heel pad. They also noted that the natural load dissipation mechanism of the skin is sufficiently effective for reducing fat pad stress and that the confinement may be undesirable.

4.2.4 High-Heel Studies

In addition to the design of sport footwear for high-performance athletes or military boots, current female trends of wearing high-heeled shoes, which affect the biomechanics of the foot, also concern researchers. Gu et al. [197] were the first authors to analyze the biomechanical effect of walking with high-heeled shoes by the FE method. They simulated the high-heeled gait and the flat-shoe gait with a 2D sagittal model; the results showed larger stresses in the metatarsus and plantar aponeurosis for the high-heel case. A more elaborated model was subsequently presented by Yu et al. [28]. They developed a 3D anatomically detailed model of the female foot with a high-heeled support. In this preliminary study, they compared experimental measurements with FE predictions of plantar pressure for flat- and high-heeled conditions for the same volunteer. In a subsequent study, they measured the plantar pressures of

twenty-four female volunteers for three heel elevations by applying four different weight-bearing conditions. The average pressure in these measurements was calculated and compared with four different heel elevation FE models [122]. In both studies, the pattern of load transfer from heel to forefoot was predicted; however, the point-to-point correspondence in the pressure distribution was not achieved. Both the experiment and the model indicated a nonlinear relationship from flat support to high-heeled support. A better match was accomplished when the model was donned with a real high-heeled shoe. This recent coupled foot–high–heeled–shoe FE model was employed to simulate the three major stance instances, as shown in Fig. 9, which enable the prediction of not only the bone and joint stresses during shod walking but also the confinement foot pressure [42].

5 Discussion

A general review of the computational studies of foot biomechanics has been presented in this paper. The results from FE models have been generally accepted for the estimation of the mechanical response of the foot in different loading and pathological conditions. A few aspects of the computational simulation of the foot are discussed here.

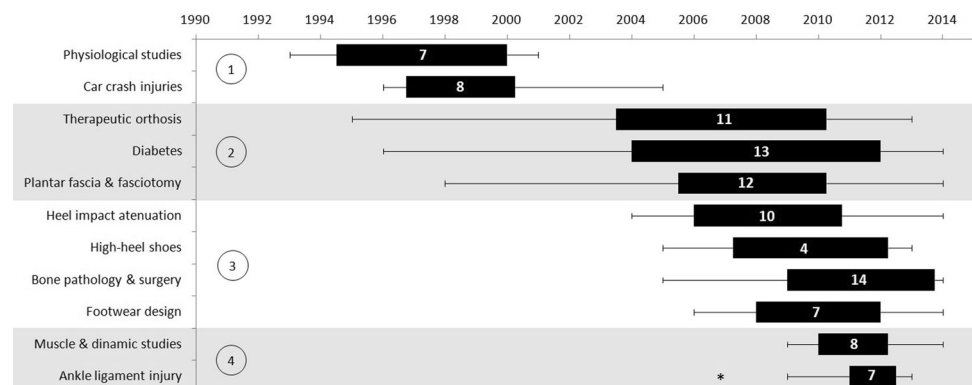
The objective of foot FE studies has evolved over the years. This evolution is depicted in Fig. 10. The first studies in the 1990s were focused on the physiological behavior of the foot. Estimations of the stress distribution in a normal foot during gait in different stance phases were habitual objectives of 2D models with strong simplifications. These papers attempted to establish the basis of foot simulations; although the majority of the results were not compared with experimental measurements, the potential application of foot FE models were realized. In subsequent years, a number of papers about car crash injuries in the foot and ankle were published. These models were

validated by comparing the FE predictions with the results of impact tests. Studies of specific topics, such as therapeutic orthosis and clinical application studies about diabetic foot and plantar fascia became prevalent. The three topics are directly related to plantar pressure under metatarsals heads and heel regions and have been continuously analyzed via modeling over the last 14 years. In these cases, the plantar pressure predicted by the FE models was compared with the experimental measurements of plantar pressure.

With this background and the maturity of the computational simulation field, new topics emerged. In 2005, researchers began to focus on more concrete applications. New branches within the following main areas were developed: clinical applications and footwear applications. In the first field, many studies of the pre- and post-surgery evaluation of bone and fascia surgeries were reported. The impact absorbing function of the heel pad were completely explored, in bare feet and coupled with footwear. The new branches of footwear focused on the biomechanics of the high-heeled gait and insole design, which were particularly oriented to sport footwear and military boots. These models are characterized by 3D detailed geometries of complete feet or partial and/or 2D models with nonlinear properties. The conclusions of these studies were much more practical with better validation processes. A better understanding of other soft tissues, in addition to fat (muscle/tendons and ligaments), was the objective of recent studies. Features of these components have been introduced in the models using more refined approaches. Dynamic studies of the foot have also been performed in recent years.

No model is capable of realistic simulation without simplifications; even with advances in computational simulation; assumptions at some level are necessary. These simplifications have evolved with advances in technology, such as computational capacity and numerical techniques, with the need to balance the geometry with the material properties and boundary conditions. In current foot FE

Fig. 10 Boxplot of the years of publication of computational foot models in different topics. Four different periods are distinguished: (1) first studies, (2) recurrent topics, (3) new topics boom 2005, (4) latest topics. The numbers over the boxes means number of papers published in that topic. Asterisk represents an outlier



models, some common simplifications are frequent. Simplifications in the geometry, such the fusion of phalanges joints, the representation of tendons and ligaments as truss elements and the simulation of the cartilage as a connecting tissue and disregarding its contact feature, are common in extremely demanding boundary condition models. When many nonlinear formulations are included in the model, simplified or partial foot shape 3D and 2D models are employed. When an accurately detailed full foot is modeled, cortical and trabecular bones are not differentiated and all tissues are simulated as linear elastic, with the exception of soft tissue that surrounds the skeleton, which is defined as bulk fat tissue with hyperelastic properties.

Regarding the mesh in foot FE simulation, the majority of the models employed a tetrahedral mesh, which is easier to automatically generate. The creation of an alternative hexahedral mesh is significantly more laborious in complex geometries, such as the foot structure, which requires user intervention. Although advances in automatic hexahedral meshing can reduce this time-intensive task [198], the tetrahedral mesh fits better in irregular geometries, where hexahedral mesh cannot be detailed with a reasonable element size. Models composed of hexahedral meshes are generally preferred; however, the literature about numerical modeling in biomechanics is inconsistent in this regard. A comparative study of tetrahedral and hexahedral FE meshes of a femur bone concluded that tetrahedral elements enabled results that are similar to the theoretical results and the use of second-order elements did not produce significant differences [199]. Conversely, a similar study that compared soft tissue contact with hyperelastic properties yielded better performance with linear hexahedral elements; however, quadratic tetrahedral mesh was qualitatively similar and may be a reasonable alternative because tetrahedral mesh generation is a highly automated process [200].

Based on the analyzed subject, some studies were unable to obtain reliable experimental data to compare the results of the simulation. In these cases, a comparison of the results with other computational models may help to determine whether the results fall within a reasonable range. This comparison is a controversial issue. Unlike comparisons with experimental data, the comparison of computational results is highly dependent on the assumptions and conditions imposed in each model. Therefore, this information should be considered in the comparison of FE results. Instead, a discussion of the conclusions from the simulations is highly recommended.

To assess stress of foot tissues, the values of von Mises stresses are frequently listed in the literature. The von Mises stress is a criterion of failure for isotropic and ductile materials. In tissue engineering, this criterion can be useful to predict pain in a component in total terms; however,

maximum principal strain criterion is preferred to predict fracture [201]. The use of von Mises stress is also inaccurate for the comparison with experimental measurements because this criterion converts the complex stress state to a single scalar numerical value. For tissues, the maximum and minimum principal stress values enable computational and experimental comparisons.

5.1 Future Directions

The large number of applications of FE analysis of the foot will continue to increase with the increased of power of computing, which doubles its computational capacity every 18 months since the invention of computing, halving costs (known as Moore's law). However, computer power will never be sufficient considering that the number of detailed geometries, complex formulations and demanding conditions will always increase. The direction of better and faster solutions is promising with vast potential for improvement. The verification and validation of FE models remains challenging. General issues of challenges and future directions in foot computational simulation are presented here.

Due to the complexity of the biomechanical behavior of the foot, many unsolved problems and challenges remain. Muscle system simulation has caused a significant barrier for the use of continuum mechanics analysis as a useful clinical diagnostic tool. Tendon activity, which is commonly modeled as equivalent forces or elastic bars, has to be simulated with real geometry to introduce active tissue behavior (muscle driven models) [118]. Similarly, a significant improvement in geometry and formulation of the skin behavior, which is frequently disregarded, is needed [144]. Another challenge of foot modeling is the bio-realistic representation and definition of the tissue properties of fascia, ligaments and cartilages, which are the first tissues simplified in complete foot applications. Despite the nonlinear nature of living tissues, all tissues in foot modeling, with the exception of fat, are generally defined by the linear elastic approach. This assumption is attributed to the complex structure of the foot and the difficulty of obtaining accurate definitions for the *in vivo* tissue properties. The material properties employed in foot models have not change since they became a useful tool for biomechanical investigations. In recent years, a number of nonlinear constitutive models have emerged: in bone, inhomogeneous density-dependent [51] and orthotropic [49] formulations, ligament fiber-reinforced visco-elastic constitutive model [97], plantar fascia, hyperelastic transversely isotropic properties [40], fat pad, visco-hyperelastic formulation [183] and skin fiber-reinforced hyperelastic constitutive model [144]. These

improvements can aid in the investigation of the fundamental biomechanical responses of the foot to improve our understanding of soft tissue disorders and to provide a sensible scientific basis to facilitate clinical diagnosis and surgical treatments.

With a well-based background of the biomechanical processes of the foot, approaches from other fields can be applied in foot simulation. Chemical processes that are dependent on the solicitations (mechanical stimulus) of an organ, such as the ulceration process [169] and the bone remodeling process [202], can be applied in foot models. Physicians and physiotherapists have become increasingly interested in dynamically exploring the entire gait. Due to the computational cost of dynamic analysis, few studies have been published. Particularly, the dynamic study by Chen et al. [136] of the heel pad impact and the plantar fascia dynamic study proposed by Lin et al. [40] are references for future studies.

Recent literature of computational simulation of the foot includes numerous full-foot subject-specific models, which require labor-intensive and time-consuming procedures. These models are based on the conclusions for one patient for the subject matter, which yields a large extrapolation. In many cases, the conclusion is dependent on the patient conditions. More valuable information would be obtained from physicians' viewpoints if computational simulations were performed for each patient, which is referred to as personalized medicine [203]. The development of a patient-specific anatomical geometry on a per-patient basis is an interesting future research direction. Spirka et al. [204] presented a simplified 3D parametric representation of metatarsals for footwear design. Simplified models are still based on patient-specific medical images but they eliminate the need for labor-intensive and time consuming segmentation and meshing procedures within an acceptable degree of accuracy for clinical practice. Some approaches have been introduced for automation of this complex and laborious process of developing anatomically accurate subject-specific models with reduced costs. Recently, a method for semi-automated patient-specific articular contact surface identification based on patient-specific bone information has been applied to the determination of articular cartilage of the first ray of the foot [205]. A patient-specific anatomical foot model that consists of the skin of the original specific model and the morphed bones of a generic model have been developed [206]. The advances in computational foot modeling will help to produce reliable simulations and analyses of foot pathologies like other computerized diagnosis systems [207] as part of the modern tools for personalized medicine.

6 Conclusions

A number of computational simulations for predicting and/or evaluating the biomechanical behavior of all aspects of the foot were reviewed. The evolution and scope of the field were outlined. The sophisticated arched bony structure of the foot makes the modeling of its mechanical response extremely challenging. This simulation is more complex when the muscle function is considered. Our major findings and conclusions are as follows:

- The foot is a complex structure that involves many different tissues and components.
- FE analysis is a complex task with the potential for errors. Thus, every effort must be made to create models that simulate the issue to a suitable degree of accuracy, especially in clinical applications.
- Simpler material properties and constitutive models are commonly used in whole foot simulation compared with studies of the biomechanics of single tissues due the computational difficulties associated with 3D modeling.
- Assumptions and simplifications at some level are necessary in computer simulation and are dependent on the objective of the study. The reasons for their adoption and their impact on the results have to be clearly explained.
- Verification and validation of the model must be performed by the authors to improve the credibility of the predictions.
- Computational foot simulations expand the knowledge of foot biomechanics, which provide meaningful information for clinical practice.
- Foot modeling is a time-consuming task, and investigations of the automation of the process will be decisive for the implementation of patient-specific studies.
- Computation foot simulations also improve the footwear design process because many different load conditions are evaluated without prefabricating samples and repeating subject trials.
- Authors have to carefully report the data and compare the results. Efforts must be made to report the results providing sufficient information of the framework of the study.
- Foot simulation is a field in constant evolution. Advances in material properties and numerical methods are forthcoming.

Acknowledgments The authors gratefully acknowledge the support of the Brazilian Government (CAPES) and of the Pró-Reitoria de Pesquisa da Universidade Federal de Minas Gerais.

References

- Saltzman C, Nawoczenski D (1995) Complexities of foot architecture as a base of support. *J Orthop Sports Phys Ther* 21:354–360
- Prendergast PJ (1997) Finite element models in tissue mechanics and orthopaedic implant design. *Clin Biomech* 12:343–366
- Mackerle J (2006) Finite element modeling and simulations in orthopedics: a bibliography 1998–2005. *Comput Methods Biomech Biomed Eng* 9:149–199
- Kirby KA (2001) What future direction should podiatric biomechanics take? *Clin Podiatr Med Surg* 18:719–723 vii
- Nakamura S, Crowninshield RD, Cooper RR (1981) An analysis of soft tissue loading in the foot—a preliminary report. *Bull Prosthet Res* 18:27–34
- Patil K, Braak L, Huson A (1996) Analysis of stresses in two-dimensional models of normal and neuropathic feet. *Med Biol Eng Comput* 34:280–284
- Lemmon D, Shiang TY, Hashmi A, Ulbrecht JS, Cavanagh PR (1997) The effect of insoles in therapeutic footwear—a finite element approach. *J Biomech* 30:615–620
- Gefen A, Megido-Ravid M, Itzchak Y, Arcan M (2000) Biomechanical analysis of the three-dimensional foot structure during gait: a basic tool for clinical applications. *J Biomech Eng* 122:630–639
- Gefen A (2002) Stress analysis of the standing foot following surgical plantar fascia release. *J Biomech* 35:629–637
- Gefen A (2003) Plantar soft tissue loading under the medial metatarsals in the standing diabetic foot. *Med Eng Phys* 25:491–499
- Jacob S, Patil MK (1999) Three-dimensional foot modeling and analysis of stresses in normal and early stage hansen's disease with muscle paralysis. *J Rehabil Res Dev* 36:252–263
- Bandak FA, Tannous RE, Toridis T (2001) On the development of an osseo-ligamentous finite element model of the human ankle joint. *Int J Solids Struct* 38:1681–1697
- Chen W, Tang F, Ju C-W (2001) Stress distribution of the foot during mid-stance to push-off in barefoot gait : a 3-D finite element analysis. *Clin Biomech* 16:614–620
- Cheung JT-M, Zhang M, An K-N (2004) Effects of plantar fascia stiffness on the biomechanical responses of the ankle-foot complex. *Clin Biomech* 19:839–846
- Cheung JT-M, Zhang M, Leung AK-L, Fan Y-B (2005) Three-dimensional finite element analysis of the foot during standing—a material sensitivity study. *J Biomech* 38:1045–1054
- Qiu T-X, Teo E-C, Yan Y-B, Lei W (2011) Finite element modeling of a 3D coupled foot-boot model. *Med Eng Phys* 33:1228–1233
- Sopher R, Nixon J, McGinnis E, Gefen A (2011) The influence of foot posture, support stiffness, heel pad loading and tissue mechanical properties on biomechanical factors associated with a risk of heel ulceration. *J Mech Behav Biomed Mater* 4:572–582
- Cheung JT, Zhang M (2006) Finite element modeling of the human foot and footwear. ABAQUS users' conference. pp 145–159
- Antunes PJ, Dias GR, Coelho AT, Rebelo F, Pereira T (2006) Non-linear finite element modelling of anatomically detailed 3D foot model. 1st ECCOMAS Thematic Conference on Computational Vision and Medical Image Processing, Oporto
- Bayod J, Becerro-de-Bengoa-Vallejo R, Losa-Iglesias ME, Doblaré M (2012) Mechanical stress redistribution in the calcaneus after autologous bone harvesting. *J Biomech* 45:1219–1226
- Flavin R, Halpin T, O'Sullivan R, FitzPatrick D, Ivankovic A, Stephens MM (2008) A finite-element analysis study of the metatarsophalangeal joint of the hallux rigidus. *J Bone Jt Surg Br* 90:1334–1340
- Chen W-M, Lee T, Lee PV-S, Lee JW, Lee S-J (2010) Effects of internal stress concentrations in plantar soft-tissue—a preliminary three-dimensional finite element analysis. *Med Eng Phys* 32:324–331
- Fontanella CG, Matteoli S, Carniel EL, Wilhelm JE, Virga A, Corvi A et al (2012) Investigation on the load-displacement curves of a human healthy heel pad: in vivo compression data compared to numerical results. *Med Eng Phys* 34:1253–1259
- Cheng H-YK, Lin C-L, Wang H-W, Chou S-W (2008) Finite element analysis of plantar fascia under stretch—the relative contribution of windlass mechanism and Achilles tendon force. *J Biomech* 41:1937–1944
- Budhabhatti SP, Erdemir A, Petre M, Sferra J, Donley B, Cavanagh PR (2007) Finite element modeling of the first ray of the foot: a tool for the design of interventions. *J Biomech Eng* 129:750–756
- García-González A, Bayod J, Prados-Frutos JC, Losa-Iglesias M, Jules KT, Becerro de Bengoa-Vallejo R et al (2009) Finite-element simulation of flexor digitorum longus or flexor digitorum brevis tendon transfer for the treatment of claw toe deformity. *J Biomech* 42:1697–1704
- Isvilanonda V, Dengler E, Iaquinto JM, Sangeorzan BJ, Ledoux WR (2012) Finite element analysis of the foot: model validation and comparison between two common treatments of the clawed hallux deformity. *Clin Biomech* 27:837–844 (Bristol, Avon)
- Yu J, Cheung JT-M, Fan Y, Zhang Y, Leung AK-L, Zhang M (2008) Development of a finite element model of female foot for high-heeled shoe design. *Clin Biomech* 23:31–38
- Qian Z, Ren L, Ren L, Boonpratatong A (2010) A three-dimensional finite element musculoskeletal model of the human foot complex. *IFMBE Proc* 31:297–300
- Babuska I, Oden JT (2004) Verification and validation in computational engineering and science: basic concepts. *Comput Methods Appl Mech Eng* 193:4057–4066
- Oreskes N, Shrader-Frechette K, Belitz K (1994) Verification, validation, and confirmation of numerical models in the earth sciences. *Science* 263:641–646
- Erdemir A, Guess TM, Halloran J, Tadepalli SC, Morrison TM (2012) Considerations for reporting finite element analysis studies in biomechanics. *J Biomech* 45:625–633
- Roache PJ (1998) Verification and validation in computational science and engineering. Hermosa Publishers, Albuquerque
- Anderson AE, Ellis BJ, Weiss JA (2007) Verification, validation and sensitivity studies in computational biomechanics. *Comput Methods Biomech Biomed Eng* 10:171–184
- Viceconti M, Olsen S, Nolte L-P, Burton K (2005) Extracting clinically relevant data from finite element simulations. *Clin Biomech* 20:451–454
- Henninger HB, Reese SP, Anderson AE, Weiss JA (2010) Validation of computational models in biomechanics. *Proc Inst Mech Eng Part H J Eng Med* 224:801–812
- Razak AHA, Zayegh A, Begg RK, Wahab Y (2012) Foot plantar pressure measurement system: a review. *Sensors* 12:9884–9912 (Basel)
- Chockalingam N, Healy A, Naemi R, Burgess-Walker P, Abdul Razak AH, Zayegh A, Begg RK, Wahab Y (2013) Comments and reply to: foot plantar pressure measurement system: a review. *Sensors* 13:3527–3529
- Guiotto A, Sawacha Z, Guarneri G, Avogaro A, Cobelli C (2014) 3D finite element model of the diabetic neuropathic foot: a gait analysis driven approach. *J Biomech* 47:3064–3071
- Lin S-C, Chen CP-C, Tang SF-T, Chen C-W, Wang J-J, Hsu C-C et al (2014) Stress distribution within the plantar aponeurosis during walking—a dynamic finite element analysis. *J Mech Med Biol* 14:1450053

41. Liu X, Zhang M (2013) Redistribution of knee stress using laterally wedged insole intervention: finite element analysis of knee-ankle-foot complex. *Clin Biomech* 28:61–67 (Bristol, Avon)
42. Yu J, Cheung JT-M, Wong DW-C, Cong Y, Zhang M (2013) Biomechanical simulation of high-heeled shoe donning and walking. *J Biomech* 46:2067–2074
43. Liang J, Yang Y, Yu G, Niu W, Wang Y (2011) Deformation and stress distribution of the human foot after plantar ligaments release: a cadaveric study and finite element analysis. *Sci China Life Sci* 54:267–271
44. Chen W-M, Park J, Park S-B, Shim VP-W, Lee T (2012) Role of gastrocnemius-soleus muscle in forefoot force transmission at heel rise—a 3D finite element analysis. *J Biomech* 45:1783–1789
45. Petre M, Erdemir A, Panoskaltis VP, Spirka TA, Cavanagh PR (2013) Optimization of nonlinear hyperelastic coefficients for foot tissues using a magnetic resonance imaging deformation experiment. *J Biomech Eng* 135:61001–61012
46. Tannous RE, Bandak FA, Toridis TG, Eppinger RH (1996) Three-dimensional finite element model of the human ankle: development and preliminary application to axial impulsive loading. *Proc Stapp Car Crash Conf* 40:219–236
47. Shin J, Yue N, Untaroiu CD (2012) A finite element model of the foot and ankle for automotive impact applications. *Ann Biomed Eng* 40:2519–2531
48. Ishii H, Sakurai Y, Maruyama T (2014) Effect of soccer shoe upper on ball behaviour in curve kicks. *Sci Rep* 4:1–8
49. Natali AN, Forestiero A, Carniel EL, Pavan PG, Dal Zovo C (2010) Investigation of foot plantar pressure: experimental and numerical analysis. *Med Biol Eng Comput* 48:1167–1174
50. Tao K, Wang D, Wang C, Wang X, Liu A, Nester CJ et al (2009) An in vivo experimental validation of a computational model of human foot. *J Bionic Eng* 6:387–397
51. Trabelsi N, Milgrom C, Yosibash Z (2014) Patient-specific FE analyses of metatarsal bones with inhomogeneous isotropic material properties. *J Mech Behav Biomed Mater* 29:177–189
52. Burkhart TA, Andrews DM, Dunning CE (2013) Finite element modeling mesh quality, energy balance and validation methods: a review with recommendations associated with the modeling of bone tissue. *J Biomech* 46:1477–1488
53. Oberkampf WL, Trucano TG, Hirsch C (2002) Verification, validation, and predictive capability in computational engineering and physics. *Found. verif. valid. 21st century work.* p 1–74, 2002
54. Currey J (2003) The many adaptations of bone. *J Biomech* 36:1487–1495
55. Cowin SC (1979) On the strength anisotropy of bone and wood. *J Appl Mech* 46:832–838
56. Wirtz D, Schiffrers N, Pandorf T (2000) Critical evaluation of known bone material properties to realize anisotropic FE-simulation of the proximal femur. *J Biomech* 33:1325–1330
57. Cowin SC, Van Buskirk WC, Ashman RB (1987). The properties of bone. *Handb Bioeng.* McGraw-Hill, New York
58. Huiskes R (1982) On the modelling of long bones in structural analyses. *J Biomech* 15:65–69
59. Wu L, Zhong S, Zheng R, Qu J, Ding Z, Tang M et al (2007) Clinical significance of musculoskeletal finite element model of the second and the fifth foot ray with metatarsal cavities and calcaneal sinus. *Surg Radiol Anat* 29:561–567
60. Evans FG (1973) Mechanical properties of bone. Thomas C.C, Springfield
61. Yamada H (1970) Strength of biological materials. The Williams & Wilkins Company, Baltimore
62. Cowin SC (1985) The relationship between the elasticity tensor and the fabric tensor. *Mech Mater* 4:137–147
63. Goldstein SA (1987) The mechanical properties of trabecular bone: dependence on anatomic location and function. *J Biomech* 20:1055–1061
64. Morgan EF, Bayraktar HH, Keaveny TM (2003) Trabecular bone modulus—density relationships depend on anatomic site. *J Biomech* 36:897–904
65. Currey J (1984) What should bones be designed to do? *Calcif Tissue Int* 36:7–8
66. Keaveny TM, Guo XE, Wachtel EF, McMahon TA, Hayes WC (1994) Trabecular bone exhibits fully linear elastic behavior and yields at low strains. *J Biomech* 27:1127–1136
67. Rho JY, Ashman RB, Turner CH (1993) Young's modulus of trabecular and cortical bone material: ultrasonic and microtensile measurements. *J Biomech* 26:111–119
68. Novitskaya E, Chen P-Y, Hamed E, Jun L, Lubarda V, Jasiuk I et al (2011) Recent advances on the measurement and calculation of the elastic moduli of cortical and trabecular bone: a review. *Theor Appl Mech* 38:209–297
69. García-Aznar JM, Bayod J, Rosas A, Larrainzar R, García-Bógaló R, Doblaré M et al (2009) Load transfer mechanism for different metatarsal geometries: a finite element study. *J Biomech Eng* 131:021011
70. Wu L (2007) Nonlinear finite element analysis for musculoskeletal biomechanics of medial and lateral plantar longitudinal arch of virtual Chinese human after plantar ligamentous structure failures. *Clin Biomech* 22:221–229
71. Helgason B, Perilli E, Schileo E, Taddei F, Brynjólfsson S, Viceconti M (2008) Mathematical relationships between bone density and mechanical properties: a literature review. *Clin Biomech* 23:135–146 (Bristol, Avon)
72. Cheung JT-M, Zhang M (2005) A 3-dimensional finite element model of the human foot and ankle for insole design. *Arch Phys Med Rehabil* 86:353–358
73. Chen W-P, Ju C-W, Tang F-T (2003) Effects of total contact insoles on the plantar stress redistribution: a finite element analysis. *Clin Biomech* 18:S17–S24
74. Van Buskirk WC, Ashman RB (1981) The elastic moduli of bone. *Mech Prop Bone ASME AMD* 45:131
75. Niu WX, Wang LJ, Feng TN, Jiang CH, Fan YB, Zhang M (2013) Effects of bone Young's modulus on finite element analysis in the lateral ankle biomechanics. *Appl Bionics Biomech* 10:189–195
76. Wakabayashi I, Itoi E, Sano H, Shibuya Y, Sashi R, Minagawa H et al (2003) Mechanical environment of the supraspinatus tendon: a two-dimensional finite element model analysis. *J Shoulder Elb Surg* 12:612–617
77. Willing RT, Lalone EA, Shannon H, Johnson JA, King GJW (2013) Validation of a finite element model of the human elbow for determining cartilage contact mechanics. *J Biomech* 46:1767–1771
78. Butz KD, Merrell G, Nauman EA (2012) A biomechanical analysis of finger joint forces and stresses developed during common daily activities. *Comput Methods Biomech Biomed Engin* 15:131–140
79. Kim J-E, Li Z, Ito Y, Huber CD, Shih AM, Eberhardt AW et al (2009) Finite element model development of a child pelvis with optimization-based material identification. *J Biomech* 42:2191–2195
80. Beillas P, Papaioannou G, Tashman S, Yang KH (2004) A new method to investigate in vivo knee behavior using a finite element model of the lower limb. *J Biomech* 37:1019–1030
81. Nguyen TC (2005) Mathematical modelling of the biomechanical properties of articular cartilage. University of Queensland, Queensland
82. Clift SE (1992) Finite-element analysis in cartilage biomechanics. *J Biomed Eng* 14:217–221
83. Thomas VJ, Patil KM, Radhakrishnan S (2004) Three-dimensional stress analysis for the mechanics of plantar ulcers in diabetic neuropathy. *Med Biol Eng Comput* 42:230–235

84. Tao K, Wang C-T, Wang D-M, Wang X (2005) Primary analysis of the first ray using a 3-dimension finite element foot model. *Conf. Proc IEEE Eng Med Biol Soc* 3:2946–2949 Shanghai, China
85. Actis RL, Ventura LB, Smith KE, Commean PK, Lott DJ, Pilgram TK et al (2006) Numerical simulation of the plantar pressure distribution in the diabetic foot during the push-off stance. *Med Biol Eng Comput* 44:653–663
86. Mak AF, Lai WM, Mow VC (1987) Biphasic indentation of articular cartilage—I. Theoretical analysis. *J Biomech* 20:703–714
87. Athanasiou KA, Liu GT, Lavery LA, Lancot DR, Schenck RC (1998) Biomechanical topography of human articular cartilage in the first metatarsophalangeal joint. *Clin Orthop Relat Res* 348:269–281
88. Schreppers GJ, Sauren AA, Huson A (1990) A numerical model of the load transmission in the tibio-femoral contact area. *Proc Inst Mech Eng H* 204:53–59
89. Moglo K, Shirazi-Adl A (2003) On the coupling between anterior and posterior cruciate ligaments, and knee joint response under anterior femoral drawer in flexion: a finite element study. *Clin Biomech* 18:751–759
90. Weiss JA, Gardiner JC (2001) Computational modeling of ligament mechanics. *Crit Rev Biomed Eng* 29:303–371
91. Peña E, Calvo B, Martínez MA, Doblaré M (2006) A three-dimensional finite element analysis of the combined behavior of ligaments and menisci in the healthy human knee joint. *J Biomech* 39:1686–1701
92. Guo Y, Zhang X, Chen W (2009) Three-dimensional finite element simulation of total knee joint in gait cycle. *Acta Mech Solida Sin* 22:347–351
93. Provenzano P, Lakes R, Keenan T, Vanderby R Jr (2001) Non-linear ligament viscoelasticity. *Ann Biomed Eng* 29:908–914
94. Peña E, Peña JA, Doblaré M (2008) On modelling nonlinear viscoelastic effects in ligaments. *J Biomech* 41:2659–2666
95. Forestiero A, Carniel EL, Natali AN (2014) Biomechanical behaviour of ankle ligaments: constitutive formulation and numerical modelling. *Comput Methods Biomech Biomed Eng* 17:395–404
96. Siegler S, Block J, Schneck CD (1988) The mechanical characteristics of the collateral ligaments of the human ankle joint. *Foot Ankle Int* 8:234–242
97. Forestiero A, Carniel EL, Venturato C, Natali AN (2013) Investigation of the biomechanical behaviour of hindfoot ligaments. *Proc Inst Mech Eng H* 227:683–692
98. Wang JH-C (2006) Mechanobiology of tendon. *J Biomech* 39:1563–1582
99. Komi P (1990) Relevance of in vivo force measurements to human biomechanics. *J Biomech* 23:23–34
100. Kongsgaard M, Aagaard P (2005) Structural Achilles tendon properties in athletes subjected to different exercise modes and in Achilles tendon rupture patients. *J Appl Physiol* 99:1965–1971
101. Lichtwark GA, Wilson AM (2005) In vivo mechanical properties of the human Achilles tendon during one-legged hopping. *J Exp Biol* 208:4715–4725
102. Kongsgaard M, Nielsen CH, Hegnsvad S, Aagaard P, Magnusson SP (2011) Mechanical properties of the human Achilles tendon, in vivo. *Clin Biomech* 26:772–777 (Bristol, Avon)
103. Peltonen J, Cronin NJ, Stenroth L, Finni T, Avela J (2012) Achilles tendon stiffness is unchanged one hour after a marathon. *J Exp Biol* 215:3665–3671
104. Louis-Ugbo J, Leeson B, Hutton WC (2004) Tensile properties of fresh human calcaneal (Achilles) tendons. *Clin Anat* 17:30–35
105. Wren TA, Yerby SA, Beaupré GS, Carter DR (2001) Mechanical properties of the human achilles tendon. *Clin Biomech* 16:245–251
106. Hansen P, Kovanen V, Hölmich P, Krogsgaard M, Hansson P, Dahl M et al (2013) Micromechanical properties and collagen composition of ruptured human achilles tendon. *Am J Sports Med* 41:437–443
107. Datta B, Salleh R, Mafulli N, Neil M, Butler A, Walsh W (2006) Mechanical properties of human flexor hallucis longus, peroneus brevis and tendo achilles tendons. 52nd annual meeting orthopaedic research society paper no 1889, p1889. 2006
108. Sebastian H, Datta B, Maffulli N, Neil M, Walsh WR (2007) Mechanical properties of reconstructed achilles tendon with transfer of peroneus brevis or flexor hallucis longus tendon. *J Foot Ankle Surg* 46:424–428
109. Severinsen K, Andersen H (2007) Evaluation of atrophy of foot muscles in diabetic neuropathy—a comparative study of nerve conduction studies and ultrasonography. *Clin Neurophysiol* 118:2172–2175
110. Hing WA, Rome K, Cameron AF (2009) Reliability of measuring abductor hallucis muscle parameters using two different diagnostic ultrasound machines. *J Foot Ankle Res* 2:33
111. Mickle KJ, Nester CJ, Crofts G, Steele JR (2013) Reliability of ultrasound to measure morphology of the toe flexor muscles. *J Foot Ankle Res* 6:12
112. Schechtman H, Bader D (1997) In vitro fatigue of human tendons. *J Biomech* 30:829–835
113. Maganaris CN, Paul JP (1999) In vivo human tendon mechanical properties. *J Physiol* 521:307–313
114. Maganaris CN, Paul JP (2002) Tensile properties of the in vivo human gastrocnemius tendon. *J Biomech* 35:1639–1646
115. Bayod J, Losa-Iglesias M, de Bengoa-Vallejo RB, Prados-Frutos JC, Jules KT, Doblare M (2010) Advantages and drawbacks of proximal interphalangeal joint fusion versus flexor tendon transfer in the correction of hammer and claw toe deformity. A finite-element study. *J Biomech Eng* 132(5):51002–51007
116. Gu YD, Li JS, Lake MJ, Ren XJ, Zeng YJ (2008) The mechanical response of Achilles tendon during different kinds of sports. *Commun Numer Methods Eng* 24:2077–2085
117. Spyrou LA (2009) Muscle and tendon tissues : constitutive modeling, numerical implementation and applications. University of Thessaly, Greece
118. Spyrou LA, Aravas N (2012) Muscle-driven finite element simulation of human foot movements. *Comput Methods Biomech Biomed Eng* 15:925–934
119. Erdemir A, Hamel AJ, Fauth AR, Piazza SJ, Sharkey NA (2004) Dynamic loading of the plantar aponeurosis in walking. *J Bone Jt Surg Am* 86:546–552
120. Kim W, Voloshin AS (1995) Role of plantar fascia in the load bearing capacity of the human foot. *J Biomech* 28:1025–1033
121. Sarrafian SK (1987) Functional characteristics of the foot and plantar aponeurosis under tibiotalar loading. *Foot Ankle Int* 8:4–18
122. Luximon Y, Luximon A, Yu J, Zhang M (2012) Biomechanical evaluation of heel elevation on load transfer—experimental measurement and finite element analysis. *Acta Mech Sin* 28:232–240
123. Hsu Y-C, Gung Y-W, Shih S-L, Feng C-K, Wei S-H, Yu C-H et al (2008) Using an optimization approach to design an insole for lowering plantar fascia stress—a finite element study. *Ann Biomed Eng* 36:1345–1352
124. Wright DG, Rennels DC (1964) A study of the elastic properties of plantar fascia. *J Bone Jt Surg Am* 46:482–492
125. Kitaoka HB, Luo ZP, Growney ES, Berglund LJ, An K-N (1994) Material properties of the plantar aponeurosis. *Foot Ankle Int* 15:557–560

126. Pavan PG, Stecco C, Darwish S, Natali NA, de Caro R (2011) Investigation of the mechanical properties of the plantar aponeurosis. *Surg Radiol Anat* 33:905–911
127. Pavan PG, Pachera P, Stecco C, Natali AN (2014) Constitutive modeling of time-dependent response of human plantar aponeurosis. *Comput Math Methods Med*. doi:10.1155/2014/530242
128. Rome K (1998) Mechanical properties of the heel pad: current theory and review of the literature. *Foot* 8:179–185
129. Miller-Young JE, Duncan NA, Baroud G (2002) Material properties of the human calcaneal fat pad in compression: experiment and theory. *J Biomech* 35:1523–1531
130. Gefen A, Megido-Ravid M, Itzchak Y (2001) In vivo biomechanical behavior of the human heel pad during the stance phase of gait. *J Biomech* 34:1661–1665
131. Spears IR, Miller-Young JE (2006) The effect of heel-pad thickness and loading protocol on measured heel-pad stiffness and a standardized protocol for inter-subject comparability. *Clin Biomech* 21:204–212 (Bristol, Avon)
132. Erdemir A, Viveiros ML, Ulbrecht JS, Cavanagh PR (2006) An inverse finite-element model of heel-pad indentation. *J Biomech* 39:1279–1286
133. Chokhandre S, Halloran JP, van den Bogert AJ, Erdemir A (2012) A three-dimensional inverse finite element analysis of the heel pad. *J Biomech Eng* 134:031002
134. Ledoux WR, Blevins JJ (2007) The compressive material properties of the plantar soft tissue. *J Biomech* 40:2975–2981
135. Natali AN, Fontanella CG, Carniel EL (2010) Constitutive formulation and analysis of heel pad tissues mechanics. *Med Eng Phys* 32:516–522
136. Chen W-M, Lee PV-S (2015) Explicit finite element modelling of heel pad mechanics in running: inclusion of body dynamics and application of physiological impact loads. *Comput Methods Biomech Biomed Eng* 18:1582–1595
137. Brilakis E, Kaselouris E, Xypnitos F, Provatidis CG, Efstathopoulos N (2012) Effects of foot posture on fifth metatarsal fracture healing: a finite element study. *J Foot Ankle Surg* 51:720–728
138. Takahashi A, Suzuki J, Takemura H (2012) Finite element modeling and simulation of human gait with a spontaneous plantar flexion. *Int J Aerosp Light Struct* 02:171–185
139. Sun P-C, Shih S-L, Chen Y-L, Hsu Y-C, Yang R-C, Chen C-S (2012) Biomechanical analysis of foot with different foot arch heights: a finite element analysis. *Comput Methods Biomech Biomed Eng* 15:563–569
140. Qian Z, Ren L, Ren L (2010) A coupling analysis of the biomechanical functions of human foot complex during locomotion. *J Bionic Eng* 7:S150–S157
141. Spears IR, Miller-Young JE, Sharma J, Ker RF, Smith FW (2007) The potential influence of the heel counter on internal stress during static standing: a combined finite element and positional MRI investigation. *J Biomech* 40:2774–2780
142. Gu Y, Li J, Ren X, Lake MJ, Zeng Y (2010) Heel skin stiffness effect on the hind foot biomechanics during heel strike. *Skin Res Technol* 16:291–296
143. Natali AN, Fontanella CG, Carniel EL (2012) Constitutive formulation and numerical analysis of the heel pad region. *Comput Methods Biomech Biomed Eng* 15:401–409
144. Fontanella CG, Carniel EL, Forestiero A, Natali AN (2014) Investigation of the mechanical behaviour of the foot skin. *Skin Res Technol* 20:445–452
145. Patil K, Braak L, Huson A (1993) A two dimensional model of a normal foot with cartilages and ligaments for stress analysis. *Innov Technol Biol Méd* 14:152–162
146. Patil KM, Braak LH, Huson A (1993) Stresses in simplified two dimensional model of a normal foot—a preliminary analysis. *Mech Res Commun* 20:1–7
147. Jacob S, Patil K, Braak L, Huson A (1996) Stresses in a 3D two arch model of a normal human foot. *Mech Res Commun* 23:387–393
148. Andrea SED, Thompson D, Cao D, Davis B (1999) Finite Element Modeling of Load Transmission Through the Calcaneus. In: 23rd annual meeting of the American Society of Biomechanics, Pittsburgh.
149. Giddings V, Beaupre G, Whalen R, Carter D (2000) Calcaneal loading during walking and running. *Med Sci Sports Exerc* 32:627–634
150. Qian Z, Ren L, Ding Y, Hutchinson JR, Ren L (2013) A dynamic finite element analysis of human foot complex in the sagittal plane during level walking. *PLoS One* 8:e79424
151. Halloran JP, Erdemir A, van den Bogert AJ (2009) Adaptive surrogate modeling for efficient coupling of musculoskeletal control and tissue deformation models. *J Biomech Eng* 131:011014
152. Halloran JP, Ackermann M, Erdemir A, van den Bogert AJ (2010) Concurrent musculoskeletal dynamics and finite element analysis predicts altered gait patterns to reduce foot tissue loading. *J Biomech* 43:2810–2815
153. Cheung JT-M, Zhang M, An K-N (2006) Effect of Achilles tendon loading on plantar fascia tension in the standing foot. *Clin Biomech* 21:194–203
154. Beaugonin M, Haug E, Cesari D (1996) Numerical model of the human ankle/foot under impact loading in inversion and eversion. *Proc Stapp Car Crash Conf* 40:239–249
155. Beaugonin M, Haug E, Cesari D (1997) Improvement of numerical ankle/foot model: modeling of deformable bone. *Proc Stapp Car Crash Conf* 41:225–237
156. Kitagawa Y, Ichikawa H, King A, Levine R (1998) A severe ankle and foot injury in frontal crashes and its mechanism. *SAE Technical Paper* 983145. doi:10.4271/983145
157. Kitagawa Y, Ichikawa H, King A, Begeman P (2000) Development of a human ankle/foot model. In: Kajzer J, Tanaka E, Yamada H (eds). *Human Biomechanics and Injury Prevention SE - 15*. Springer, Japan, pp 117–22
158. Iwamoto M, Mikki K, Tanaka E (2005) Ankle skeletal injury predictions using anisotropic inelastic constitutive model of cortical bone taking into account damage evolution. *Stapp Car Crash J* 49:133–156
159. Beillas P, Lavaste F, Nicolopoulos D, Kayventash K, Yang KH, Robin S (1999) Foot and ankle finite element modeling using ct-scan data. 43rd Stapp Car Crash Conf., San Diego (CA), pp 217–42, 1999
160. Liacouras PC, Wayne JS (2007) Computational modeling to predict mechanical function of joints: application to the lower leg with simulation of two cadaver studies. *J Biomech Eng* 129:811–817
161. Liu Q, Zhang K, Zhuang Y, Li Z, Yu B, Pei G (2013) Analysis of the stress and displacement distribution of inferior tibiofibular syndesmosis injuries repaired with screw fixation: a finite element study. *PLoS One* 8:e80236
162. Wei F, Hunley SC, Powell JW, Haut RC (2011) Development and validation of a computational model to study the effect of foot constraint on ankle injury due to external rotation. *Ann Biomed Eng* 39:756–765
163. Wei F, Braman JE, Weaver BT, Haut RC (2011) Determination of dynamic ankle ligament strains from a computational model driven by motion analysis based kinematic data. *J Biomech* 44:2636–2641
164. Gu YD, Ren XJ, Li JS, Lake MJ, Zhang QY, Zeng YJ (2010) Computer simulation of stress distribution in the metatarsals at

- different inversion landing angles using the finite element method. *Int Orthop* 34:669–676
165. Spears I, Miller-Young J, Waters M, Rome K (2005) The effect of loading conditions on stress in the barefooted heel pad. *Med Sci Sports Exerc* 37:1030–1036
 166. Cavanagh P, Erdemir A, Petre M (2008) A finite element approach to examine the relationship between plantar pressure and internal stress in the foot. In: 54th Annual Meeting of the Orthopaedic Research Society. San Francisco, CA
 167. Chen W, Lee P, Lee S (2009) Investigation of plantar barefoot pressure and soft-tissue internal stress: a three-dimensional finite element analysis. *13th Int Conf Biomed Eng IFMBE Proc* 23:1817–1820
 168. Fernandez JW, Ul Haque MZ, Hunter PJ, Mithraratne K (2012) Mechanics of the foot Part 1: a continuum framework for evaluating soft tissue stiffening in the pathologic foot. *Int J Numer Method Biomed Eng* 28:1056–1070
 169. Sciumè G, Boso DP, Gray WG, Cobelli C, Schrefler BA (2014) A two-phase model of plantar tissue: a step toward prediction of diabetic foot ulceration. *Int J Numer Method Biomed Eng* 30:1153–1169
 170. Wong DW-C, Zhang M, Yu J, Leung AK-L (2014) Biomechanics of first ray hypermobility: an investigation on joint force during walking using finite element analysis. *Med Eng Phys* 36:1388–1393
 171. Gefen A, Megido-Ravid M, Itzchak Y, Arcan M (1998) In: Proceedings of Medicon'98 VIII Mediterranean Conference on Medical and Biological Engineering and Computing, Lemesos (Limassol), Cyprus, 14–17 June 1998
 172. Cheung JT, An KN, Zhang M (2006) Consequences of partial and total plantar fascia release: a finite element study. *Foot Ankle Int Am Orthop Foot Ankle Soc Swiss Foot Ankle Soc* 27:125–132
 173. Tao K, Ji W-T, Wang D-M, Wang C-T, Wang X (2010) Relative contributions of plantar fascia and ligaments on the arch static stability: a finite element study. *Biomed Tech* 55:265–271 (Berl)
 174. Iaquinio JM, Wayne JS (2010) Computational model of the lower leg and foot/ankle complex: application to arch stability. *J Biomech Eng* 132:021009
 175. Matzaroglou C, Bougas P, Panagiotopoulos E, Saridis A, Karanikolas M, Kouzoudis D (2010) Ninety-degree chevron osteotomy for correction of hallux valgus deformity: clinical data and finite element analysis. *Open Orthop J* 4:152–156
 176. Bayod J, de Bengoa Vallejo RB, Losa Iglesias ME, Dobaré M (2013) Stress at the second metatarsal bone after correction of hammertoe and claw toe deformity: a finite element analysis using an anatomical model. *J Am Podiatr Med Assoc* 103:260–273
 177. Wang Y, Li Z, Zhang M (2014) Biomechanical study of tarsometatarsal joint fusion using finite element analysis. *Med Eng Phys* 36:1394–1400
 178. Jordan C, Bartlett R (1995) Pressure distribution and perceived comfort in casual footwear. *Gait Posture* 3:215–220
 179. Witana CP, Goonetilleke RS, Xiong S, Au EYL (2009) Effects of surface characteristics on the plantar shape of feet and subjects' perceived sensations. *Appl Ergon* 40:267–279
 180. Erdemir A, Saucerman JJ, Lemmon D, Loppnow B, Turso B, Ulbrecht JS et al (2005) Local plantar pressure relief in therapeutic footwear: design guidelines from finite element models. *J Biomech* 38:1798–1806
 181. Actis RL, Ventura LB, Lott DJ, Smith KE, Commean PK, Hastings MK et al (2008) Multi-plug insole design to reduce peak plantar pressure on the diabetic foot during walking. *Med Biol Eng Comput* 46:363–371
 182. Gu YD, Li JS, Lake MJ, Zeng YJ, Ren XJ, Li ZY (2011) Image-based midsole insert design and the material effects on heel plantar pressure distribution during simulated walking loads. *Comput Methods Biomech Biomed Eng* 14:747–753
 183. Fontanella CG, Forestiero A, Carniel EL, Natali AN (2013) Analysis of heel pad tissues mechanics at the heel strike in bare and shod conditions. *Med Eng Phys* 35:441–447
 184. Lin S, Lin C, Tang F, Chen W (2007) Combining experimental material property test and finite element analysis to investigate the plantar foot pressure distribution during standing. *J Biomech* 40:S337–S338
 185. Chu TM, Reddy NP, Padovan J (1995) Three-dimensional finite element stress analysis of the polypropylene, ankle-foot orthosis: static analysis. *Med Eng Phys* 17:372–379
 186. Chu TM, Reddy NP (1995) Stress distribution in the ankle-foot orthosis used to correct pathological gait. *J Rehabil Res Dev* 32:349–360
 187. Goske S, Erdemir A, Petre M, Budhabhatti S, Cavanagh PR (2006) Reduction of plantar heel pressures: insole design using finite element analysis. *J Biomech* 39:2363–2370
 188. Cheung JT, Zhang M (2008) Parametric design of pressure-relieving foot orthosis using statistics-based finite element method. *Med Eng Amp Phys* 30:269–277
 189. Luo G, Houston VL, Garbarini MA, Beattie AC, Thongpop C (2011) Finite element analysis of heel pad with insoles. *J Biomech* 44:1559–1565
 190. Lin S-Y, Su K-C, Chang C-H (2013) Reverse engineering of CT-based rocker sole model—finite element analysis. *1st IntConf Orange Technol*. doi:10.1109/ICOT.2013.6521151
 191. Cheung JT-M, Yu J, Wong DW-C, Zhang M (2009) Current methods in computer-aided engineering for footwear design. *Footwear Sci* 1:31–46
 192. Verdejo R, Mills NJ (2004) Heel-shoe interactions and the durability of EVA foam running-shoe midsoles. *J Biomech* 37:1379–1386
 193. Even-Tzur N, Weisz E, Hirsch-Falk Y, Gefen A (2006) Role of EVA viscoelastic properties in the protective performance of a sport shoe: computational studies. *Biomed Mater Eng* 16:289–299
 194. Cho J-R, Park S-B, Ryu S-H, Kim S-H, Lee S-B (2009) Landing impact analysis of sports shoes using 3-D coupled foot-shoe finite element model. *J Mech Sci Technol* 23:2583–2591
 195. Dai X-Q, Li Y, Zhang M, Cheung JT-M (2006) Effect of sock on biomechanical responses of foot during walking. *Clin Biomech* 21:314–321
 196. Bates KT, Savage R, Pataky TC, Morse SA, Webster E, Falkingham PL, Ren L, Qian Z, Collins D, Bennett MR, McClymont J, Crompton RH (2013) Does footprint depth correlate with foot motion and pressure? *J R Soc Interface*. doi:10.1098/rsif.2013.0009
 197. Gu Y, Li J (2005) Finite element analysis of the instep fatigue trauma in the high-heeled gait. *World J Model Simul* 1:117–122
 198. Liewers WB, Kent RW (2013) Patient-specific modelling of the foot: automated hexahedral meshing of the bones. *Comput Methods Biomech Biomed Eng* 16:1287–1297
 199. Ramos A, Simões JA (2006) Tetrahedral versus hexahedral finite elements in numerical modelling of the proximal femur. *Med Eng Phys* 28:916–924
 200. Tadepalli SC, Erdemir A, Cavanagh PR (2011) Comparison of hexahedral and tetrahedral elements in finite element analysis of the foot and footwear. *J Biomech* 44:2337–2343
 201. Schileo E, Taddei F, Cristofolini L, Viceconti M (2008) Subject-specific finite element models implementing a maximum principal strain criterion are able to estimate failure risk and fracture location on human femurs tested in vitro. *J Biomech* 41:356–367
 202. Idhammad A, Abdali A, Alaa N (2013) Computational simulation of the bone remodeling using the finite element method: an elastic-damage theory for small displacements. *Theor Biol Med Model* 10:32

203. Pokorska-Bocci A, Stewart A, Sagoo GS, Hall A, Kroese M, Burton H (2014) “Personalized medicine”: what’s in a name? *Pers Med* 11:197–210
204. Spirka TA, Erdemir A, Ewers Spaulding S, Yamane A, Telfer S, Cavanagh PR (2014) Simple finite element models for use in the design of therapeutic footwear. *J Biomech* 47:2948–2955
205. Marchelli GLS, Ledoux WR, Isvilanonda V, Ganter MA, Storti DW (2014) Joint-specific distance thresholds for patient-specific approximations of articular cartilage modeling in the first ray of the foot. *Med Biol Eng Comput* 52:773–779
206. Lochner SJ, Huissoon JP, Bedi SS (2014) Development of a patient-specific anatomical foot model from structured light scan data. *Comput Methods Biomech Biomed Engin* 17:1198–1205
207. Podshivalov L, Fischer A, Bar-Yoseph PZ (2014) On the road to personalized medicine: multiscale computational modeling of bone tissue. *Arch Comput Methods Eng* 21:399–479